Medicinal Chemistry Research
https://doi.org/10.1007/s00044-020-02605-5

MEDICINAL CHEMISTRY RESEARCH

ORIGINAL RESEARCH

Synthesis, molecular docking, α-glucosidase inhibition, and antioxidant activity studies of novel benzimidazole derivatives

Gagandeep Singh[1] · Amanjot Singh[1] · Varinder Singh[1] · Raman K. Verma[1] · Jyoti Tomar[1] · Rajiv Mall[2]

Received: 31 March 2020 / Accepted: 23 July 2020

Abstract

A novel series of *N*-methyl/benzyl-substituted benzimidazolyl-linked *para*-substituted benzyl-based compounds containing 2,4-thiazolidinediones, dimethyl malonate (DMM), and diethyl malonate (DEM) **17**–**27** were designed, docked, synthesized, and evaluated for their antidiabetic activity studies. Structures of all the synthesized compounds were confirmed through ^{1}H NMR, ^{13}C NMR, FTIR, and mass spectrometry. Four targeted compounds (**17**–**18** and **22**–**23**) showed good inhibitory potential in the range of 4.10 ± 0.01 to 9.12 ± 0.06 μM. Furthermore, synthesized compounds **17**–**27** were evaluated for their antioxidant potential and compared with standard ascorbic acid and results showed that compound **18** (EC_{50} = 0.176 ± 0.002 mM) being the most active. Compounds **17**–**18** and **22**–**23** exhibited prominent antidiabetic as well as antioxidant activity. Compound **18** was considered a promising candidate for this series. The designed molecules were docked into α-glucosidase protein (PDB Code. 3TOP) to develop a correlation with the α-glucosidase inhibition studies and were also additionally docked into PPARγ proteins (PDB ID: 2PRG) with rosiglitazone (standard drug) to study their PPARγ binding affinity in comparison with rosiglitazone and to classify these compounds for their PPARγ agonistic behavior.

Keywords Molecular docking · α-Glucosidase inhibition · Antioxidant · PPARγ · Rosiglitazone · Acarbose

Introduction

Diabetes is a metabolic disorder escalating in the world population at an alarming rate (Albrecht et al. 2010). Non-insulin-dependent type-2 diabetes mellitus (T2DM) accounts for more than 90% of the cases. It is characterized by insulin resistance in the liver and peripheral tissues. One way to tackle the underlying causes for T2DM would be to increase the sensitivity of tissues and therefore the body's response to insulin (Liu et al. 2011). Peroxisome proliferator-activated receptors (PPARs) are transcription factors that belong to the nuclear receptor family. The three PPAR subtypes PPARα, PPARδ, and peroxisome proliferator-activated receptors γ (PPARγ) play an important role in glucose and lipid homeostasis (Berger and Moller 2002). Agonists of the γ subtype have been studied for their role in regulating glucose metabolism and insulin sensitivity. One of the oldest metabolic disorders is diabetes mellitus (DM). DM is characterized by pathologically higher blood sugar levels due to or insulin resistance or insulin secretion failure.

Diabetes is a chronic metabolic disorder characterized by hyperglycemia in which an elevated level of glucose circulates in blood plasma. This hike in glucose level is either because the pancreas is not producing much insulin or the cells do not respond to secreted insulin (West 2000). Therefore to treat diabetes, a therapeutic approach is to decrease postprandial hyperglycemia by inhibiting the carbohydrate hydrolyzing enzymes α-amylase and α-glucosidase (Chakrabarti and Rajagopalan 2002).

α-Glucosidase is a membrane-bound enzyme located in the epithelium of the human small intestine and is a key enzyme in carbohydrate digestion. It hydrolyzes the terminal, non-reducing 1,4-linked α-D-glucose residues with release of α-D-glucose and helps digestion and absorption

Supplementary information The online version of this article (https://doi.org/10.1007/s00044-020-02605-5) contains supplementary material, which is available to authorized users.

✉ Rajiv Mall
rajivmall@pbi.ac.in

[1] Synthetic Organic and Medicinal Chemistry Laboratory, Department of Chemistry, Punjabi University, Patiala, 147002 Punjab, India

[2] Department of Basic and Applied Sciences, Punjabi University, Patiala, 147002 Punjab, India

Published online: 01 August 2020

of sugars. α-glucosidase inhibitors can be used as a first-line drug for the treatment of type-2 diabetes because they can lower the rate of carbohydrate absorption and suppression of postprandial hyperglycemia.

Recently, a more effective strategy for the treatment of T2DM has involved the disturbance of dietary monosaccharide absorption by inhibition of α-glucosidase (Kim et al. 2014). Also, the latest review (Dhameja and Gupta 2019) entitled "Synthetic heterocyclic candidates as promising α-glucosidase inhibitors: An overview" reporting α-glucosidase enzyme inhibition is an effective therapeutic decorum in the treatment of T2DM. Since 1990, carbohydrate mimics Acarbose, voglibose and miglitol are in clinical use that bind reversibly itself to α-glucosidase and discontinue the saccharide hydrolysis. Side effects of using these drugs are mainly gastrointestinal which include nausea, bloating, diarrhea, abdominal pain, and flatulence (Yee and Fong 1996; Kaku 2014; Scott and Spencer 2000; Mizuno et al. 2008).

To overcome these side effects, and long synthetic routes to access them forced the researchers to move their focus to discover simple and small heterocyclic motifs that work as promising α-glucosidase inhibitors and may eventually lead to the management of the postprandial hyperglyc1emic condition in T2DM (Zhang et al. 2017).

In this regard, this review deals with synthetic heterocyclic derivatives and hybrids for α-glucosidase inhibition with structure–activity relationship (SAR) studies along with interactions displayed from docking results; wherever available from the literature.

Even the mechanistic and physiological studies of α-glucosidase enzyme inhibition are well reported and documented. In the digestion and absorption process of carbohydrates pancreatic α-amylase hydrolysis the starch (Gray 1975). Moreover, α-amylase as the most abundant enzyme in the human saliva, it performs several distinct functions in the oral cavity. First, it breaks the carbohydrates in the oral cavity and second, it binds to viridans streptococci in the oral cavity. Bacteria-bound α-amylase hydrolyzes the starch molecules. The α-glycosidase enzyme plays a key role in intestinal carbohydrates digestion, glycogen degradation, maturation, and glycoprotein folding (Ghani 2015). Inhibitors of these enzymes reduce starch hydrolysis to simple sugars by slowing the action of these enzymes (Notkins 2002).

Because of their deleterious side effects, such as abdominal distention, bloating, and diarrhea, the efforts for finding and synthesis of new effective and safer inhibitors have continued (Zawawi et al. 2016). Review of literature revealed that benzimidazole and its derivatives exhibit a wide spectrum of biological and pharmacological activities (Akhtar et al. 2017) including antidiabetics (Verma et al. 2013a, 2012a, 2012b, 2013b, 2015; Özil et al. 2016a, 2016b, 2016c; Wang et al. 2017a; Tahaa et al. 2016) also. Current studies from literature revealed that thiazolidinediones (TZDs) and its derivatives are effective chemotherapeutic agents that can act as a new class of α-glucosidase inhibitors (Chinthala et al. 2013; Wang et al. 2017b).

This chronic hyperglycemia may lead to increased oxidative stress in patients with diabetes and plays a key role in the various long-term complications, such as retinopathy, neuropathy, nephropathy, and cardiovascular disease (Hirose et al. 2017). Also, in DM, α-glucosidase is a membrane-bound enzyme found in the epithelium of the human small intestine and is a key enzyme in carbohydrate digestion.

α-Glucosidase inhibitors can be used as a first-line drug for the treatment of type-2 diabetes because they can lower the rate of carbohydrate absorption and suppression of postprandial hyperglycemia.

Oxidative stress concerning the risk factors for coronary artery disease (CAD) before the late advanced symptoms has been important in recent research. Oxidative stress is defined as an imbalance between the production of reactive oxygen species or free radicals and antioxidant defense, which may induce tissue injury.

In diabetes, oxidative stress is caused by both an increased formation of plasma-free radicals and a reduction in antioxidant defenses. Hyperinsulinemia and hyperglycemia may enhance the production of free radicals and induce oxidative stress that may also contribute to increased risk for CAD in diabetes (Ceriell 2000). An unbalanced excess of free oxygen radicals due to lack of antioxidants may increase the risk of CAD.

PPARs are ligand-activated transcription factors belonging to the nuclear hormone receptor superfamily, which are the most important receptors involved in the treatment of type-2 diabetes. PPARγ are molecular target of the TZDs such as pioglitazone and rosiglitazone act as PPARγ full agonists, play a key role in adipogenesis activation to improve glucose metabolism and insulin sensitivity for control hyperglycemia (Ibrahim et al. 2017; Vallvee et al. 2015). Unfortunately, PPARγ full agonists showed various adverse effects including renal fluid retention, adipogenesis, bone fracture, weight gain, and increased incidence of cardiovascular events (Guasch et al. 2011). On the other hand, compounds with low transactivation activity for PPARγ, called selective PPARγ modulators or PPARγ partial agonists such as s26948 (Carmona et al. 2007), retain very good antidiabetic effects without these undesired side effects. Therefore, several partial agonists of PPARγ are being developed as new-antidiabetic drugs (Guasch et al. 2011).

Benzimidazole derivatives exhibit a wide range of pharmaceutical and biological activities including α-glucosidase inhibitors (Ozil et al. 2016a, 2016b; Dinparast et al.

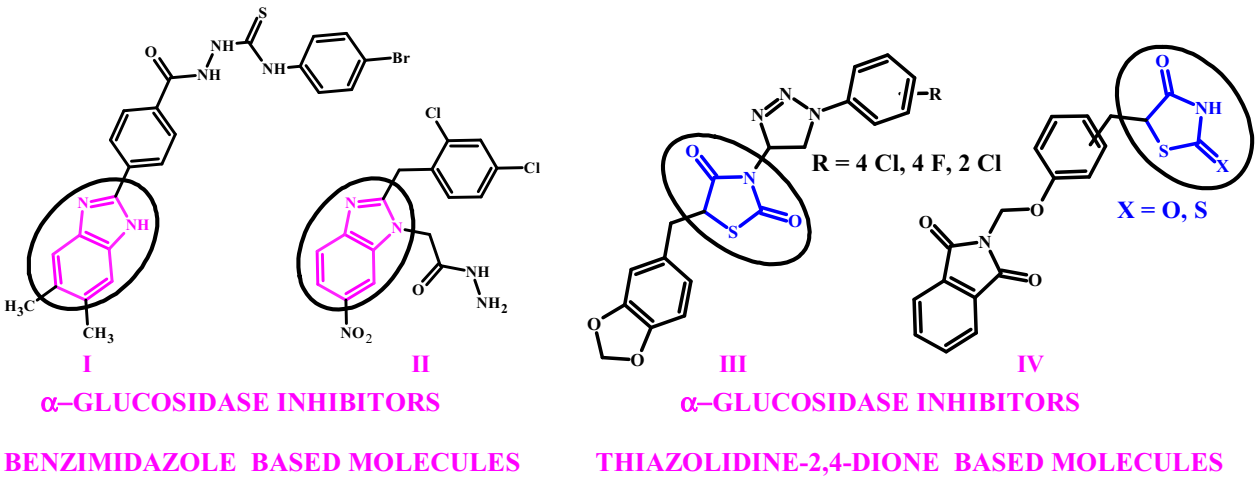

Fig. 1 The structures of drugs and pharmacologically active compounds

2016; Zawawi et al. 2017; Arshad et al. 2016; Zawawi et al. 2016) [compound **I** (Zawawi et al. 2017) and **II** (Ozil et al. 2016b) (Fig. 1)] and antioxidant (Mavrova et al. 2015; Menteşe et al. 2015). Thiazolidine-2,4-diones and their cyclic/acyclic analogs (DMM and DEM) are important moieties due to their broad range of biological activities, including antidiabetic and α-glucosidase inhibitors (Chinthala et al. 2013; Wang et al. 2017) and antioxidant (Rekha and Chandrashekhara 2015). Recently, Chinthala et al. (2013) [**III** (Fig. 1)] and Wang et al. (2017) [**IV** (Fig. 1)] have reported that a novel series of thiazolidine-2,4-dione derivatives act as a new class of α-glucosidase inhibitors. Also, recent studies have shown that multiple activating compounds with combined α-glucosidase inhibition and antioxidant activities are more effective therapeutics in DM treatment (Rekha and Chandrashekhara 2015; Shahidpour et al. 2015). From the literature survey, we revealed that molecules containing benzimidazole and TZD or their acyclic analogs (DMM and DEM) have gained a huge interest as potent antidiabetic drugs. So, it would be interesting to hybridize (Fig. 2) these dynamic frameworks into a single molecular motif to act as α-glucosidase inhibitors along with antioxidant active novel compounds. We have already explored a different series of heterocyclic compounds including benzimidazole for their potential therapeutic effects (Yousefi et al. 2015; Kaur et al. 2018; Singh et al. 2018a, b; Singh et al. 2017, 2018a, b; Mall et al. 2019). Keeping the importance of benzimidazole and TZDs in our minds, we in this study designed and synthesized a novel series of *N*-methyl/benzyl benzimidazolyl para-substituted benzyl-based molecules containing three pharmacologically potent hydrogen-bonding parts (TZD, DMM, and DEM) with **-NH-** or **-CH_2NH-** linkers (**17**–**27**) according to literature protocol. The biological activities of novel synthesized molecules were evaluated in terms of α-glucosidase inhibition along with antioxidant activity and which is further supported by the molecular docking studies.

Material and methods

General

All the chemicals used in the reported work were purchased from Sigma-Aldrich and SD Fine chemicals without further purification. The melting/boiling points reported here were recorded using an open concentrated sulfuric acid bath and are uncorrected. TLC analysis was carried out on glass plates coated with silica gel-GF254 (Loba Chemie), and spots were visualized using a UV cabinet (Perfit India). Column chromatography was performed using silica gel 60–120 mesh (Loba Chemie). ^{1}H, ^{13}C, NMR spectra were recorded on a Bruker AVANCE II 400 (400.13, 100.62 MHz) NMR spectrometer, BrukerBioSpin, Switzerland. Chemical shifts were reported in ppm (δ) with reference to the internal standard TMS. The signals were designated as follows: br broad, s singlet, d doublet, t triplet, m multiplet. Molecular weights of the synthesized compounds were checked by (LC-MS) Waters, Q-TOF Micromass, UK in ESI mode and GC-MS (Shimadzu). The Infrared of the reported compounds were recorded on Perkin Elmer Spectrum RX FT-IR FTIR Spectrophotometer, USA.

Compounds **1**–**4** although novel, were and previously reported from our laboratory (Singh et al. 2017, 2018a, b; Mall et al. 2019; Najafi et al. 2012; Musialik and Litwinienko 2005; Musialik et al. 2009; Verma et al. 2013a). Synthetic procedures and spectral characterization data for all these compounds are available in the supplementary material.

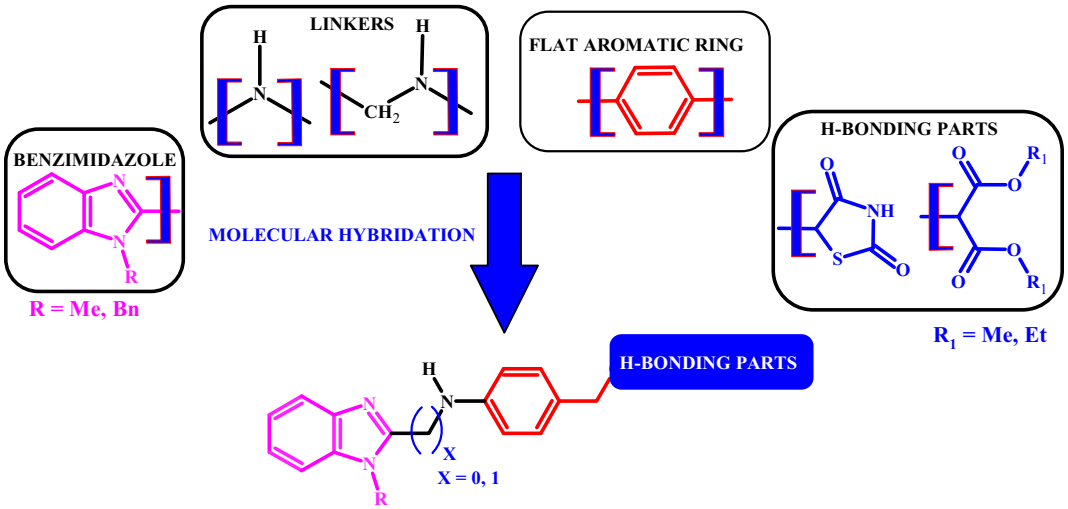

Fig. 2 Design of new chemical entities (NCEs) containing benzimidazole and thiazolidinediones

Chemistry

Procedure for the synthesis of N-benzyl-2-nitroaniline 5

The mixture of o-nitroaniline (1.0 g, 0.0072 mol) and benzyl bromide (1.49 g, 0.0087 mol, 1.2 equiv.) in water (20 mL) was stirred magnetically at 100 °C (oil bath) for 2 h. The reaction was monitored by TLC. The reaction mixture was cooled to room temperature and treated with $NaHCO_3$ and extracted with EtOAc (3 × 5 mL) dried ($MgSO_4$) and concentrated under reduced pressure. The crude product was subjected to column chromatography using silica gel (60–120 mesh) as solid phase and hexane/EtOAc as mobile phase to obtain pure **5**. Yield 1.84 g, 84%; m. p. 73–75 °C; ^{1}H NMR (400 MHz, DMSO-d_6): δ 8.64 (*t*, 1H, $J = 5.76$ Hz, –N–**H**), 8.09 (dd, 1H, $J = 1.56$, 8.60 Hz, Ar–**H**), 7.42 (*m*, 5H, Ar–**H**), 7.27 (*m*, 1H, Ar–**H**), 6.87 (*d*, 1H, $J = 8.00$ Hz, Ar–**H**), 6.67 (*m*, 1H, Ar–**H**), 4.62 (*d*, 2H, J = 6.04 Hz, benzylic); ^{13}C-NMR (100 MHz, DMSO-d_6): δ 144.82 (C-1), 138.20 (C-5), 136.12 (C-1′), 131.30 (C-2), 128.43 (2C, C-3′ and C-5′), 126.95 (C-3), 126.77 (2C, C-2′ and C-6′), 126.08 (C-4′), 115.21 (C-4), 114.63 (C-6), 45.82 (benzylic); FTIR (neat, cm^{-1}) ν_{max}: 3397 (N–H), 3084 and 3052 (C–H, aromatic), 3027 and 2927, (C–H, aliphatic), 1618 (O=N=O, asymmetric), 1348 (O=N=O, symmetric); GC–MS (*m/z*) = 228 $[M]^+$; anal. calcd. (%) for $C_{13}H_{12}N_2O_2$: C, 68.41; H, 5.30; N, 12.27. Found: C, 66.12; H, 5.84; N, 11.96.

Procedure for the synthesis of *N*-benzylbenzene-1, 2-diamine 6

The stirred solution of *N*-benzyl-2-nitroaniline (**5**) (2.0 g, 0.00876 m) in ethanol (50 mL), $SnCl_2.2H_2O$ was added and the reaction mixture was heated under reflux for 2 h. The solvent was evaporated under reduced pressure. The residue was dissolved in saturated aqueous $NaHCO_3$ solution (100 mL) and product extracted with hot ethyl acetate (5 × 50 mL). The combined organic extracts were washed with brine (2 × 50 mL), dried over Na_2SO_4 and the solvent under reduced pressure to get desired product (**6**). Yield 1.4 g, 80.9%; m. p. 123–125 °C; ^{1}H NMR (400 MHz, DMSO-d_6): δ 7.37 (*d*, 2H, $J = 7.28$ Hz, Ar–**H**), 7.30 (*t*, 2H, $J = 7.68$ Hz, Ar–**H**), 7.21 (*t*, 1H, $J = 7.24$ Hz, Ar–**H**), 6.60 (dd, 1H, $J =$ 1.84, 7.28 Hz, Ar–**H**), 6.47 (*m*, 2H, Ar–**H**), 6.38 (dd, 1H, $J = 2.08$, 7.24 Hz, Ar–**H**), 4.92 (br s, 1H, –N–**H**), 4.39 (br s, 2H, –N**H$_2$**), 4.29 (*s*, 2H, benzylic); ^{13}C-NMR (100 MHz, DMSO-d_6): δ 140.12 (C-1), 135.81 (C-5), 134.87 (C-2), 128.04 (2C, C-3′ and C-), 127.09 (2C, C-2′ and C-6′), 126.43 (C-1′), 117.89 (C-4′), 117.08 (C-3), 114.54 (C-4), 110.40 (C-6), 47.19 (C, benzylic); FTIR (neat, cm^{-1}) ν_{max}: 3331 (N–H), 3028 and 3052 (C–H, aromatic), 2844 (C–H, aliphatic); GC–MS (*m/z*) = 198 $[M]^+$; anal. calcd. (%) for $C_{13}H_{14}N_2$: C, 78.75; H, 7.12; N, 14.13. Found: C, 78.20; H, 7.81; N, 14.13.

General procedure for the synthesis of 7 and 8

A mixture of *N*-benzylbenzene-1,2-diamine (**6**)/*N*-methylbenzene-1,2-diamine (1 mol) and chloroacetic acid (3 mol) was refluxed for 4 h in 45 mL of 4 N HCl and then cooled to room temperature and adjusted to pH = 7 with ammonia. The crudes were obtained and purification by column chromatography on silica gel mesh 60–120 eluting with ethyl acetate/hexane gave compound **7/8**, respectively.

1-benzyl-2-(chloromethyl)-1*H*-benzimidazole (7) Yield 0.90 g, 71.4%; m. p. 146−148 °C; ^{1}H NMR (400 MHz,

$CDCl_3$): δ 7.74 (*d*, 1H, $J = 6.48$ Hz, Ar–**H**), 7.27 (*m*, 6H, Ar–**H**), 7.05 (dd, 1H, $J = 1.48$, 4.32 Hz, Ar–H), 5.44 (*s*, 2H, benzylic), 4.69 (*s*, 2H, –C**H$_2$**–Cl); ^{13}C-NMR (100 MHz, $CDCl_3$): δ 164.66 (C-1), 129.12 (2C, C-3a and C-7a), 128.21 (C1′), 126.39 (C-2′ and C-6′), 123.94 (2C, C-3′ and C-5′), 122.87 (C-4′), 120.40 (2C, C-5 and C-6), 110.14 (2C, C-4 and C-7), 47.19 (C, benzylic), 37.01 (–**C**H$_2$–Cl); FTIR (neat, cm^{-1}) ν_{max}: 3024 and 3006 (C–H, aromatic), 2976 and 2926 (C–H, aliphatic), 736 (C–Cl); GC–MS (*m/z*) = 256 $[M]^+$; anal. calcd. (%) for $C_{15}H_{13}ClN_2$: C, 70.18; H, 5.10; N, 13.81. Found: C, 71.12; H, 5.33; N, 13.25.

2-(chloromethyl)-1-methyl-1*H*-benzimidazole (8) Yellow solid; yield 3.37 g, 58.60%; m. p. 133−135 °C; ^{1}H NMR (400 MHz, DMSO-d_6): δ 8.05 (td, 2H, $J = 7.52$ Hz, Ar–**H**), 7.72 (td, 2H, $J = 10.54$ Hz, Ar–**H**), 6.43 (*s*, 2H, –C**H$_2$**–Cl–), 4.08 (*s*, 3H, –C**H$_3$**); ^{13}C-NMR (100 MHz, DMSO-d_6): δ 149.14 (C-2), 140.91 (C-3a), 135.58 (C-7a), 123.10 (C-4), 122.17 (C-7), 118.97 (C-5), 110.01 (C-6), 36.51 (–**C**H$_2$–Cl), 29.95 (N–**C**H$_3$); FTIR (neat, cm^{-1}) ν_{max}: 3057 (C–H, aromatic), 2942 (C–H, aliphatic), 741 (C–Cl); GC–MS (*m/z*) = 180 $[M]^+$; anal. calcd. (%) for $C_9H_9ClN_2$: C, 59.34; H, 5.02; N, 15.51. Found: C, 60.12; H, 4.89; N, 15.02.

Procedure for the synthesis of compound Ethyl-2-bromo-3-(4-nitrophenyl)propanoate 9

The mixture of 4-nitroaniline (4.0 g, 0.029 mol) in methanol (30 mL) and acetone (30 mL), cooled to −10 °C, was added 48% aqueous HBr (13.40 mL, 0.116 mol). The mixture was stirred at 0 °C for 5 min, and a solution of sodium nitrite (2.155 g, 0.0312 mol) in water (5 mL) was added dropwise to keep the reaction temperature below 5 °C. The mixture was stirred at 0–5 °C for 15 min, and then ethyl acrylate (17.18 mL, 0.172 mol) was added dropwise. The mixture was warmed to 38 °C, powdered copper(I) oxide (0.89 g, 0.0625 mol) was added, and the mixture was stirred for 1 h, then made basic with concentrated aqueous ammonia, and extracted with ethyl acetate (2×). The combined extracts were washed with water (2×) and brine, dried over magnesium sulfate and concentrated. The pure product was isolated by column chromatography (hexane/ethyl acetate). Yellow solid; yield 5.70 g, 65.14%; m. p. 141–144 °C; ^{1}H NMR (400 MHz, $CDCl_3$): δ 8.19 (dd, 2H, $J = 1.96$, 6.80 Hz, Ar–**H**), 7.42 (dd, 2H, $J = 1.88$, 6.96 Hz, Ar–**H**), 4.43 (*t*, 1H, $J = 7.68$, 15.32 Hz, –CH$_2$–C**H**Br–COOCH$_2$CH$_3$), 4.25 (*m*, 2H, –CH$_2$–CHBr–COOC**H$_2$**CH$_3$), 3.60 (dd, 1H, $J = 7.68$, 14.28 Hz, –**H**CH–CHBr–COOCH$_2$CH$_3$), 3.38 (dd, 1H, $J = 7.60$, 14.28 Hz, –HC**H**–CHBr–COOCH$_2$CH$_3$), 1.27 (*t*, 3H, $J = 7.20$, 14.28 Hz, –CH$_2$–CHBr–COOCH$_2$C**H$_3$**); ^{13}C NMR (100 MHz, $CDCl_3$): δ 168.85 (–CH$_2$–CHBr–**C**OOCH$_2$CH$_3$), 147.25 (C-4), 144.17 (C, C-1), 130.22 (C-2 and C-6), 123.86 (C-3 and C-5), 62.41 (–CH$_2$–CHBr–COO**C**H$_2$CH$_3$), 44.23 (–CH$_2$–**C**HBr–COOCH$_2$CH$_3$), 40.50 (–**C**H$_2$–CHBr–COOCH$_2$CH$_3$), 13.90 (–CH$_2$–CHBr–COOCH$_2$**C**H$_3$); FTIR (KBr, cm^{-1}): 3077 (C–H, aromatic), 2984 and 2846 (C–H, aliphatic), 1716 (C=O), 1514 (O=N=O, asymmetric), 1344 (O=N=O, symmetric), 851 (C–Br); GC–MS (*m/z*) = 305 $[M+3]^+$. anal. calcd. (%) for $C_{11}H_{12}BrNO_4$: C, 43.73; H, 4.00; N, 4.64. Found: C, 45.11; H, 4.25; N, 4.78.

Procedure for the synthesis of compound 2-Imino-5-(4-nitrobenzyl)-1,3-thiazolidin-4-one 10

To a solution ethyl-2-bromo-3-(4-nitrophenyl)propanoate (9) (2.0 g, 0.00662 mol) in methanol (20 ml), thiourea (0.504 g, 0.00662 mol) and sodium acetate (0.543 g, 0.00662 mol) were added and heated under stirring to reflux for 6–7 h. The reaction was complete as indicated by TLC. The reaction mixture is cooled to 0–5 °C followed by filtration of the precipitated solid. The precipitates were washed with water (2 × 50 ml) and finally a few times with acetone and dried at 70–75 °C. White solid; yield 1.495 g, 89.89%; m.p. 250–255 °C; ^{1}H NMR (400 MHz, DMSO-d_6): δ 8.76 (broad *s*, 2H, N–**H**, = N–**H** of ring, both protons disapeared on D_2O exchange), 8.11 (*d*, 2H, $J = 1.80$, 8.72 Hz, Ar–**H**), 7.47 (*d*, 2H, $J = 8.60$ Hz, Ar–**H**), 4.54 (dd, 1H, $J = 4.32$, 9.04 Hz, C**H** of ring), 3.51 (dd, 1H, $J = 4.28$, 14.08 Hz, H–C–**H**, methylene), 3.13 (dd, 1H, $J = 9.04$, 14.08 Hz, **H**–C–H, methylene); ^{13}C NMR (100 MHz, DMSO-d_6): δ 188.35 (C, C=O), 181.10 (C, C=N), 146.37 (C-1), 145.95 (C-4), 130.15 (C-2 and C-6), 123.09 (C-3 and C-5), 56.97 (**C**H of ring), 38.11 (–**C**H$_2$–, methylene). FTIR (neat, cm^{-1}) ν_{max}: 3381 and 3313 (N–H), 2928 and 2668, (C–H), 1738 (C=O), 1689 (C=N), 1515 (O=N=O, asymmetric), 1310 (O=N=O, symmetric); anal. calcd. (%) for $C_{10}H_9N3O_3S$: C, 47.80; H, 3.61; N, 16.72. Found: C, 47.23; H, 4.02; N, 16.43.

Procedure for synthesis of compound 5-(4-nitrobenzyl)-1,3-thiazolidine-2,4-dione 11

2-Imino-5-(4-nitrobenzyl)-1,3-thiazolidin-4-one (**10**) (1.495 g, 0.0059 mol) and 2 N hydrochloric acid (50 ml) is heated to reflux for 6 h. After cooling to room temperature, pH of the reaction mixture is adjusted to about with aqueous sodium hydroxide solution. The precipitated solid is filtered and washed with water and dried. Fluffy white solid; Yield 1.69 g, 84.16%; m. p. 168–170 °C; ^{1}H NMR (400 MHz, DMSO-d_6): δ 11.99 (broad *s*, 1H, N**H** of TZD, disapeared on D_2O exchange), 8.13 (*d*, 2H, $J = 8.64$ Hz, Ar–**H**), 7.47 (d, 2H, $J = 8.56$ Hz, Ar–**H**), 4.77 (dd, 1H, $J = 4.48$, 8.80 Hz, C**H** of TZD), 3.53 (dd, 1H, $J = 4.52$, 14.12 Hz, H–C–**H**, methylene), 3.22 (*d*, 1H, $J = 19$ Hz, **H**–C–H,

methylene); ^{13}C NMR (100 MHz, DMSO-d_6): δ 153.77 (C-1), 144.31 (C-4), 130.28 (C-2 and C-6), 123.20 (C-3 and C-5), 51.62 (**C**H of TZD), 37.24 (–**C**H_2–TZD); FTIR (KBr, cm^{-1}) ν_{max}: 3249 (N–H), 3112 (C–H, aromatic), 1756 (4 C=O of TZD), 1742 (2 C=O of TZD), 1698 (O=N=O, asymmetric), 1345 (O=N=O, symmetric); GC–MS (*m/z*) = 252 $[M]^+$; anal. calcd. (%) for $C_{10}H_8N_2O_4S$: C, 47.61; H, 3.20; N, 11.11. Found: C, 47.20; H, 3.12; N, 11.11.

Procedure for the synthesis of compound 5-(4-aminobenzyl)-1,3-thiazolidine-2,4-dione 12

A solution of compound **11** (1.00 g, 0.004 mol) in methanol was shaken in the presence of 10% Pd–C (212 mg) in a Parr Hydrogenator under 25 psi H_2 pressure at room temperature for 12 h. The mixture was filtered through celite, and the filtrate was evaporated under reduced pressure. The residue upon recrystallization from methanol gave compound **12**. Off white solid; yield 0.807 g, 92.43%; m. p. 135–137 °C; ^{1}H NMR (400 MHz, DMSO-d_6): δ 8.71 (*s*, 2H, N**H$_2$** disapeared on D_2O exchange), 8.54 (*s*, 1H of TZD, disapeared on D_2O exchange), 6.86 (dd, 2H, J = 2.52, 10.84 Hz, 2H, Ar–**H**), 6.50 (dd, 2H, J = 3.84, 8.16 Hz, 2H, Ar–**H**), 4.37 (*m*, 1H, **H**–C of TZD ring), 3.26 (dd, 1H, J = 3.84, 14.12 Hz, H–C–**H**, methylene), 2.73 (dd, 1H, J = 9.92, 14.08 Hz, H–C–**H** methylene); ^{13}C NMR (100 MHz, DMSO-d_6): δ 189.04 (4-**C**=O of TZD), 181.60 (2-**C**=O of TZD), 146.47 (C-4), 129.10 (C-1), 125.68 (C-2, C-6), 129.10 (C-1), 113.99 (C-3, C-5), 59.11 (**C**H of TZD), 38.04 (–**C**H_2–TZD); GC–MS (*m/z*) = 222 $[M]^+$; anal. calcd. (%) for $C_{10}H_{10}N_2O_2S$: C, 54.04; H, 4.53; N, 12.60. Found: C, 54.93; H, 4.13; N, 12.11.

General procedure for the synthesis 13 and 14

A mixture of 2.5 g of 4-nitrobenzaldehyde (2.0 g, 0.0132 mol) and dimethyl malonate/diethyl malonate (0.0132 mol) and few drops of piperidinium acetate (catalytic amount) in 10 mL of toluene was refluxed for 12 h. The Dean-Stark water separator was used for the continuous removal of water. The mixture was cooled to room temperature and pure product was isolated by column chromatography (hexane/ethyl acetate).

Dimethyl(4-nitrobenzylidene)malonate (13) White solid; yield 1.56 g, 44.44%; m. p. 120–125 °C; ^{1}H NMR (400 MHz, $CDCl_3$): δ 8.25 (dd, 2H, J = 1.80, 8.80 Hz, Ar–**H**), 7.80 (*s*, 1H, benzylidenic), 7.59 (*d*, 2H, J = 8.68 Hz, Ar–**H**), 3.88 [s, 3H, (–CH=CH–(**C**OOC**H$_3$**)$_2$], 3.84 [s, 3H, (–CH=CH–(**C**OOC**H$_3$**)$_2$]; ^{13}C NMR (100 MHz, $CDCl_3$): δ 166.01 [2C, –CH=CH–(**C**$OOCH_3$)$_2$], 163.70 [–CH=CH–(**C**$OOCH_3$)$_2$], 148.51 [–**C**H=CH–(COOCH_3)$_2$], 139.95 (C-4), 139.09 (C-1), 129.90 (C-2 and C-6), 129.24 [–CH=**C**H–(COOCH_3)$_2$], 124.00 (C-3 and C-5), 53.04 [-CH=CH–(COO**C**H_3)$_2$], 52.96 [–CH=CH–(COO**C**H_3)$_2$; ESI–MS (*m/z*) = 288.15 $[M+Na]^+$; anal. calcd. (%) for $C_{12}H_{11}NO_6$: C, 54.34; H, 4.18; N, 5.28. Found: C, 54.39; H, 4.19; N, 5.85.

Diethyl(4-nitrobenzylidene)malonate (14) White solid; yield 2.66 g, 70%; m. p. 78–80 °C; ^{1}H NMR (400 MHz, $CDCl_3$): δ 8.25 (d, 2H, J = 8.84 Hz, Ar–**H**), 7.76 (s, 1H, benzylidenic), 7.62 (d, 2H, J = 8.76 Hz, Ar–**H**), 4.36 [two overlapped quartets, 4H, two (–CH=C–COOC**H$_2$**–CH_3)$_2$], 1.37 [*t*, 3H, J = 7.16 Hz, (–CH=C–$COOCH_2$–C**H$_3$**)$_2$], 1.30 [*t*, 3H, J = 7.16 Hz, (–CH=C–$COOCH_2$–C**H$_3$**)$_2$]; ^{13}C NMR (100 MHz, $CDCl_3$): δ 165.10 [–CH=C–(**C**$OOCH_2CH_3$)$_2$], 162.92 [–CH=C–(**C**$OOCH_2CH_3$)$_2$], 148.10 (C-4), 139.32 (C-2 and C-4), 138.75 [–**C**H=C–(COOCH_2CH_3)$_2$], 130.32 [–CH=**C**–(COOCH_2CH_3)$_2$], 129.01 (C-1), 123.97 (C-3 and C-5), 61.80 [–CH=C–(COO**C**H_2CH_3)$_2$], 61.78 [–CH=C–(COO**C**H_2CH_3)$_2$], 13.88 [–CH=C–(COOCH_2**C**H_3)$_2$], 13.60 [–CH=C–(COOCH_2**C**H_3)$_2$]; FTIR (KBr, cm^{-1}) ν_{max}: 2985 (C–H), 1727 (C=O), 1521 (O=N=O asymmetry), 1346 (O=N=O asymmetry O=N=O symmetry); ESI–MS (*m/z*) = 316.20 $[M+Na]^+$; GC–MS (*m/z*) = 293 $[M]^+$. anal. calcd. (%) for $C_{14}H_{15}NO_6$: C, 57.34; H, 5.16; N, 4.78. Found: C, 57.83; H, 4.90; N, 4.85.

General procedure for synthesis 15 and 16

A solution of compound **13/14** (0.011 mol) in methanol (30 ml) was shaken in the presence of 10% Pd–C (585 mg, 0.0055 mol) in a Parr Hydrogenator under 25 psi H_2 pressure at room temperature for 12 h. The mixture was filtered through celite, and the filtrate was evaporated under reduced pressure. The residue upon recrystallization from methanol gave pure compounds **15/16**, respectively.

Dimethyl(4-aminobenzyl)malonate (15) White solid; yield 1.60 g, 89.38%; 80–83 °C; ^{1}H NMR (400 MHz, $CDCl_3$): δ 6.98 (dd, 2H, J = 1.76, 6.60 Hz, Ar–**H**), 6.60 (dd, 2H, J = 1.96, 6.40 Hz, Ar–**H**), 3.68 (*s*, 6H, two –O–C**H$_3$**), 3.62 [*m*, 3H, overlapped peaks of N**H$_2$** (disapeared on D_2O exchange) + –**H**C–(COOCH_3)$_2$], 3.11 (*d*, 2H, J = 7.80 HZ, –C**H$_2$**–); ^{13}C NMR (100 MHz, DMSO-d_6): δ 169.40 [2C, –CH=CH–(**C**$OOCH_3$)$_2$], 145.10 (C-4), 129.66 (C2 and C6), 127.57 (C-1), 115.28 (C-3 and C-5), 52.48 (–**C**H_2–), 34.08 [2C, –CH=CH–(COO**C**H_3)$_2$]; IR (KBr, cm^{-1}): 3458, 3375 (N–H), 3005, 2954, 2851 (C–H), 1734 (C=O), 1281 (C–O–C); anal. calcd. (%) for $C_{12}H_{13}NO_4$: C, 61.27; H, 5.57; N, 5.95. Found: C, 60.56; H, 5.42; N, 6.12.

Diethyl(4-aminobenzyl)malonate (16) White viscous mass; yield 1.45 g, 80%; ^{1}H NMR (400 MHz, $CDCl_3$): δ = 6.99 (dd, 2H, J = 1.80, 8.36 Hz, Ar–**H**), 6.60 (dd, 2H,

$J = 1.88$, 6.52 Hz, Ar–**H**), 4.19 [two overlapped quartets, 4H, two (–CH_2=CH–COO**C**H_2–CH_3)$_2$], 3.69 (*m*, 3H, overlapped peaks of N**H**$_2$ (disapeared on D_2O exchange) + (–CH_2=C**H**–$COOCH_2$–CH_3)$_2$, 3.10 (*d*, 2H, $J = 7.88$ Hz, (–C**H**$_2$ =CH–$COOCH_2$–CH_3)$_2$, 1.23 (*t*, 6H, $J = 7.08$, 14.28 Hz, two, (–CH_2=CH–$COOCH_2$–C**H**$_3$)$_2$; ^{13}C NMR (100 MHz, $CDCl_3$): δ 169.04 [2C, (–CH_2=CH–**C**$OOCH_2$–CH_3)$_2$], 145.06 (C-4), 129.71 (C-2 and C-4), 127.71 (C-1), 115.21 (C-3 and C-5), 61.34 [2C, (–CH_2= CH–COOC**H**$_2$–CH_3)$_2$], 14.03 [2C, (–CH_2=CH–$COOCH_2$–C**H**$_3$)$_2$]; 3470, 3377 (N–H), 2982, 2938 (C–H), 1728 (C=O), 1288 (C–O–C); anal. calcd. (%) for $C_{14}H_{17}NO_4$: C, 63.87; H, 6.51; N, 5.32. Found: C, 63.02; H, 5.90; N, 5.04.

General procedure for synthesis 17–27

A solution of **3**, **4**, **7**, and **8** (1 mol), and **12**, **15**, and **16** (1.2 mol) in anhydrous ethanol (50 mL) was heated in a microwave reactor at 150 °C for 20 min. The resulting products (**17**–**27**) were purified with recrystallization or by column chromatography (ethyl acetate/ hexane).

5-{4-[(1-methyl-1*H*-benzimidazol-2-yl)amino]benzyl}-1,3-thiazolidine-2,4-dione (17) Pure white solid product was obtained by recrystallization in methanol; yield 0.093 g, 57.05%; m. p. 198–200 °C; ^{1}H NMR (400 MHz, DMSO-d_6): δ 12.00 (*s*, 1H, N–**H** of TZD), 10.68 (*s*, 1H, N–**H** of linker), 7.58 (*m*, 1H, Ar–**H**), 7.50 (*m*, 1H, Ar–**H**), 7.45 (*m*, 3H, Ar–**H**), 7.39 (*m*, 2H, Ar–**H**), 7.06 (*m*, 1H, Ar–**H**), 4.79 (dd, 1H, $J = 4.24$, 8.92 Hz, **H**–C of TZD ring), 3.58 (*s*, 3H, –C**H**$_3$), 3.52 (dd, 1H, $J = 3.88$, 13.88 Hz, **H**–C–H, methylene), 3.25 (*d*, $J = 9.04$ Hz, **H**–C–H, methylene). ^{13}C NMR (100 MHz, DMSO-d_6): δ 175.11 (4-C=O of TZD), 170.99 (2-C=O of TZD), 147.83 (C-2), 134.97 (C-1′), 134.83 (C-3a), 131.10 (C-7a), 130.60 (C-4′), 123.73 (C-6), 123.36 (C-3′ and C-5′), 123.17 (C-5), 122.63 (C-2′ and C-6′), 121.97 (C-4), 120.73 (C-7), 52.36 (**C**H of TZD), 36.96 (–**C**H_2–TZD), 29.83 (N–**C**H_3); FTIR (KBr, cm^{-1}) ν_{max}: 3422, 3391 (N–H), 1740, 1701(C=O), 1316 (C–N); ESI–MS (*m/z*) = 353 $[M+1]^+$; anal. calcd. (%) for $C_{18}H_{16}N_4O_2S$: C, 61.35; H, 4.58; N, 15.90. Found: C, 59.24; H, 4.90; N, 15.14.

5-{4-[(1-benzyl-1*H*-benzimidazol-2-yl)amino]benzyl}-1,3-thiazolidine-2,4-dione (18) Pure white solid product was obtained by recrystallization in methanol. Yield 0.044 g, 57.89%; m. p. 173–175 °C; ^{1}H NMR (400 MHz, DMSO-d_6): δ 12.05 (*s*, 1H, N–**H** of TZD), 10.78 (*s*, 1H, N–**H** of linker), 7.52 (*d*, 2H, $J = 8.24$ Hz Ar–**H**), 7.43 (*m*, 9H, Ar–**H**), 7.32 (*m*, 2H, Ar–**H**), 5.61 (*s*, 2H, benzylic protons), 4.93 (dd, 1H, $J = 4.32$, 9.08 Hz, **H**–C of TZD ring), 3.49 (dd, 1H, $J = 9.20$, 13.92 Hz, –**H**–C–H, methylene), 3.22 (dd, 1H, $J = 9.20$, 13.92 Hz, H–C–**H**, methylene). IR (KBr, cm^{-1}): 3036, 2988 (C–H), 1752, 1696 (C=O), 1251 (C–O–C). ESI–MS (*m/z*) = 428 $[M]^+$; anal. calcd. (%) for $C_{24}H_{20}N_4O_2S$: C, 67.27; H, 4.70; N, 13.07. Found: C, 68.12; H, 5.02; N, 14.21.

Dimethyl{4-[(1-methyl-1*H*-benzimidazol-2-yl)amino]benzyl} malonate (19) Pure product was obtained by column chromatography; yield 0.015 g, 61.53%; m. P. 223–225 °C; ^{1}H NMR (400 MHz, DMSO-d_6): δ 12.98 (broad *s*, 1H, N–**H** of linker), 7.61 (*d*, 1H, $J = 7.48$ Hz, Ar–**H**), 7.39 (*m*, 7H, Ar–**H**), 3.92 [*t*, 1H, $J = 7.88$, –CH_2–**H**C–($COOCH_3$)$_2$], 3.80 (*s*, 3H, –C**H**$_3$), 3.66 [*s*, 6H, two –CH_2–HC–(COOC**H**$_3$)$_2$], 3.19 (*d*, 2H, $J = 7.88$ Hz); ^{13}C NMR (100 MHz, DMSO-d_6): δ 168.61 [2C, –CH_2–CH–(**C**$OOCH_3$)$_2$], 148.04 (C-2), 134.57 (C-1′), 131.25 (C-4′), 130.14 (3a and 7a), 123.74 (C-3′ and C-5′), 123.42 (C-5 and C-6), 112.09 (C-4 and C-7), 110.20 (C-2′ and C-6′), 52.47 [–CH_2–H**C**–($COOCH_3$)$_2$], 52.32 [2C, –CH_2–HC–(COO**C**H_3)$_2$], 33.50 [–**C**H_2–HC–($COOCH_3$)$_2$], 29.82 (N–**C**H_3); IR (KBr, cm^{-1}): 3377 (N–H), 3005, 2955 (C–H), 1732 (C=O), 1250 (C–O–C). ESI–MS (*m/z*) = 367 $[M]^+$; anal. calcd. (%) for $C_{20}H_{21}N_3O_4$: C, 65.38; H, 5.76; N, 11.44. Found: C, 65.97; H, 5.12; N, 11.56.

Diethyl{4-[(1-methyl-1*H*-benzimidazol-2-yl)amino]benzyl} malonate (20) Pure product was obtained by column chromatography. Yield: .048 g, 61.53%; m. p. 198–200 °C; ^{1}H NMR (400 MHz, DMSO-d_6): δ 13.04 (broad *s*, 1H, N–**H** of linker), 7.57 (*d*, 1H, $J = 7.48$ Hz, Ar–**H**), 7.38 (*m*, 6H, Ar–**H**), 7.33 (*m*, 1H, Ar–**H**), 4.18 [two overlapped quartets, 4H, two (–CH_2–HC–(COOC**H**$_2$–CH_3)$_2$], 3.81 [dd, 1H, $J =$ 2.72, 7.76 Hz, –CH_2–C**H**–($COOCH_2$–CH_3)$_2$], 3.20 (*d*, 2H, $J = 7.80$ Hz, –C**H**$_2$–CH–($COOCH_2$–CH_3)$_2$), 1.22 [two overlapped *t*, 6H, –CH_2–CH–($COOCH_2$–C**H**$_3$)$_2$]; ^{13}C NMR (100 MHz, DMSO-d_6): δ 168.00 [2C, –CH_2–CH–(**C**$OOCH_3$)$_2$], 147.90 (C-2), 134.33 (C-1′), 131.08 (C-4′), 130.13 (3a and 7a), 123.80 (C-3′ and C-5′), 123.45 (C-5 and C-6), 112.02 (C-4 and C-7), 110.04 (C-2′ and C-6′), 60.92 [2C, –CH_2–HC–(COO**C**H_2CH_3)$_2$], 52.74 [–CH_2–H**C**–($COOCH_2CH_3$)$_2$], 33.42 [–**C**H_2–HC-($COOCH_2CH_3$)$_2$], 29.84 (N–**C**H_3), 13.78 [2C, –CH_2–HC–($COOCH_2$**C**H_3)$_2$]; IR (KBr, cm^{-1}): 3438 (N–H), 3043, 2974 (C–H), 1738 (C=O), 1246 (C–O–C); ESI–MS (m/z) = 395 $[M]^+$; anal. calcd. (%) for $C_{22}H_{25}N_3O_4$: C, 66.82; H, 6.37; N, 10.63. Found: C, 67.15; H, 6.87; N, 11.02.

Diethyl{4-[(1-benzyl-1*H*-benzimidazol-2-yl)amino]benzyl} malonate (21) Pure product was obtained by column chromatography; yield 0.039 g, 53.85%; ^{1}H NMR (400 MHz, DMSO-d_6): δ 7.78 (*d*, 2H, $J = 8.56$ Hz, Ar–**H**), 7.39 (*d*, 1H, $J = 7.64$ Hz, Ar–**H**), 7.31 (dd, 2H, $J = 7.56$,

14.6 Hz, Ar–**H**), 7.24 (*d*, 1H, $J = 7.20$ Hz, Ar–**H**), 7.17 (*m*, 5H, Ar–**H**), 7.03 (*m*, 1H, Ar–**H**), 5.50 (*s*, 2H, benzylic protons), 4.14 [two overlapped quartets, 4H, (–CH_2–HC–COOC**H**$_2$–CH_3)**$_2$**], 3.68 [*t*, 1H, $J = 7.76$ Hz, –CH_2–C**H**–($COOCH_2$–CH_3)$_2$], 3.08 [*d*, 2H, $J = 7.84$ Hz, –C**H$_2$**–CH–($COOCH_2$–CH_3)$_2$, methylene], 1.21 [*t*, 6H, $J = 7.08$ Hz –CH_2–CH–($COOCH_2$–C**H$_3$**)**$_2$**]; ^{13}C NMR (100 MHz, DMSO-d_6): δ 168.18 [2C, –CH_2–CH–(**C**OOCH_3)$_2$], 150.22 (C-2), 141.92 (C-1″), 139.28 (C-4″), 136.76 (3a and 7a), 133.41 (C-1′), 130.08 (C-2 and C-6), 128.71 (C-3′ and C-5′), 128.41 (C-3″ and C-5″), 126.45 (C-6″), 120.86 (C-2″), 119.59 (C-7), 118.01 (C-4), 116.13 (C-6), 108.25 (C-5), 60.74 (2C, –CH_2–HC–COO**C**H_2–CH_3)$_2$)], 53.30 [–CH_2–H**C**–($COOCH_2CH_3$)$_2$], 33.49 [–**C**H_2–HC–($COOCH_2CH_3$)$_2$], 29.01 (N–**C**H_2–C_6H_5), 13.78 [2C, –CH_2–HC–($COOCH_2$**C**H_3)**$_2$**]; IR (KBr, cm^{-1}): 3432 (N–H), 2974, 2876 (C–H), 1639 (C=O); ESI–MS (m/z) = 472 $[M+1]^+$; anal. calcd. (%) for $C_{28}H_{29}N_3O_4$: C, 71.32; H, 6.20; N, 8.91. Found: C, 69.80; H, 6.96; N, 9.38.

5-(4-{[(1-methyl-1*H*-benzimidazol-2-yl)methyl]amino}benzyl)-1,3-thiazolidine-2,4-dione (22) Pure white solid product was obtained by recrystallization in methanol; yield 0.062 g, 47.32%; m. p. 173–175 °C; ^{1}H NMR (400 MHz, DMSO-d_6): δ 7.61 (*d*, 1H, $J = 7.76$ Hz, Ar–**H**), 7.46 (*d*, 1H, $J = 7.68$ Hz, Ar–**H**), 7.23 (*m*, 2H, Ar–**H**), 6.95 (*d*, 2H, $J =$ 8.40 Hz, Ar–**H**), 6.70 (*d*, 2H, $J = 8.40$ Hz, Ar–**H**), 6.06 (*t*, 1H, $J = 5.08$ Hz, –CH_2–N–**H** of linker), 4.52 (d, 2H, $J =$ 5.36 Hz, –C**H$_2$**–N–H of linker), 4.24 (dd, 1H, $J = 3.28$, 10.20 Hz, **H**–C of TZD ring), 3.83 (*s*, 3H, –C**H$_3$**), 3.29 (dd, 1H, $J = 3.44$, 14.80 Hz, **H**–C–H), 2.68 (dd, $J = 10.64$, 13.88 Hz, **H**–C–H); FTIR (KBr, cm^{-1}) ν_{max}: 3428 (N–H), 2949 (C–H Ar), 2855, 2843 (C–H) 1642 (C=O); ESI–MS (m/z) = 367 $[M+1]^+$; anal. calcd. (%) for $C_{19}H_{18}N_4O_2S$: C, 62.28; H, 4.95; N, 15.29. Found: C, 63.02; H, 4.96; N, 15.11.

5-(4-{[(1-benzyl-1*H*-benzimidazol-2-yl)methyl]amino}benzyl)-1,3-thiazolidine-2,4-dione (23) Pure white solid product was obtained by recrystallization in methanol. Yield 0.062 g, 47.32%; m. p. 173–175 °C; ^{1}H NMR (400 MHz, DMSO-d_6): δ 7.65 (*m*, 1H, Ar–H), 7.41 (*m*, 1H, Ar–H), 7. 37 (*m*, 4H, Ar–H), 7.20 (*m*, 3H, Ar–H), 6.91 (*d*, 2H, $J =$ 8.40 Hz, Ar–**H**), 6.62 (*d*, 2H, $J = 8.48$ Hz, Ar–**H**), 6.15 (*t*, 1H, $J = 5.36$ Hz, –CH_2–N–**H** of linker), 5.59 (*s*, 2H, benzylic), 4.49 (*d*, 2H, $J = 5.48$ Hz, –C**H$_2$**–N–H of linker), 4.12 (dd, 1H, $J = 3.24$, 10.60 Hz, **H**–C of TZD ring), 3.26 (dd, 1H, $J = 3.48$, 10.04 Hz, **H**–C–H), 2.54 (dd, 1H, $J =$ 2.52, 9.00 Hz, **H**–C–H); FTIR (KBr, cm^{-1}) ν_{max}: 3422 and 3391 (N–H), 3069 and 3028 (C–H), 1740 (C=O), 1701 (C=O) and 1618 (C=N); ESI–MS (m/z) = 443 $[M+1]^+$; anal. calcd. (%) for $C_{25}H_{22}N_4O_2S$: C, 67.85; H, 5.01; N, 12.66. Found: C, 68.23; H, 5.66; N, 13.02.

Dimethyl(4-{[(1-methyl-1*H*-benzimidazol-2-yl)methyl]amino}benzyl)malonate (24) Pure product in white viscous form was obtained by column chromatography; Yield 0.063 g, 56.25%; ^{1}H NMR (400 MHz, DMSO-d_6): δ 7.60 (*d*, 1H, $J = 7.48$ Hz, Ar–**H**), 7.45 (*d*, 1H, $J = 7.52$ Hz, Ar–**H**), 7.24 (*m*, 2H, Ar–**H**), 6.91 (*d*, 2H, $J = 8.44$ Hz, Ar–**H**), 6.69 (*d*, 2H, $J = 8.52$ Hz, Ar–**H**), 6.04 (*t*, 1H, –CH_2–N–**H** of linker), 4.52 (*d*, 2H, $J = 5.12$ Hz, –CH_2–N–**H** of linker), 3.83 (*s*, 3H, –CH_3), 3.65 (*t*, 1H, $J = 7.60$ Hz, –CH_2–**H**C–(COO–CH_3)$_2$), 3.61 [*s*, 6H, –CH_2–CH–(COO–C**H$_3$**)**$_2$**], 2.96 (*d*, 2H, $J = 7.68$ Hz, –C**H$_2$**–CH–(COO–CH_3)$_2$); IR (KBr, cm^{-1}): 3402 (N–H), 2948, 2837 (C–H), 1647 (C=O); ESI–MS (m/z) = 382 $[M+1]^+$; anal. calcd. (%) for $C_{21}H_{23}N_3O_4$: C, 66.13; H, 6.08; N, 11.02. Found: C, 66.78; H, 6.66; N, 11.82.

Dimethyl(4-{[(1-benzyl-1*H*-benzimidazol-2-yl)methyl]amino}benzyl)malonate (25) Pure product in white viscous form was obtained by column chromatography; yield 0.073 g, 41.01%; ^{1}H NMR (400 MHz, $CDCl_3$): δ 7.81 (dd, 1H, $J = 0.88$, 8.24 Hz, –CH_2–N–**H** of linker), 7.30 (*m*, 7H, Ar–H), 7.06 (dd, 2H, $J = 2.76$, 7.68 Hz, Ar–**H**), 7.01 (dd, 2H, $J = 1.60$, 6.88 Hz, Ar–**H**), 6.60 (dd, 2H, $J = 2.20$, 8.60 Hz, Ar–**H**), 5.42 (*s*, 2H, benzylic), 4.45 (*s*, 2H, –C**H$_2$**–NH– of linker), 3.69 [*s*, 3H, –CH_2–CH–(COO–C**H$_3$**)$_2$], 3.68 (*s*, 3H, –CH_2–CH–(COO–C**H$_3$**)$_2$), 3.59 [*t*, 1H, $J = 7.72$ Hz, –CH_2–**H**C–(COO–CH_3)$_2$], 3.11 [*d*, 2H, $J = 7.80$ Hz, –C**H$_2$**–CH–(COO–CH_3)$_2$]; IR (KBr, cm^{-1}): 3441 (N–H), 2960 and 2930 (C–H), 1726 (C=O) and 1623 (C=N). ESI–MS (m/z) = 457 $[M]^+$; anal. calcd. (%) for $C_{27}H_{27}N_3O_4$: C, 70.88; H, 5.95; N, 9.18. Found: C, 69.33; H, 5.02; N, 10.21.

Diethyl(4-{[(1-methyl-1*H*-benzimidazol-2-yl)methyl]amino}benzyl)malonate (26) Pure product was obtained by column chromatography; yield 0.052 g, 44.06%; ^{1}H NMR (400 MHz, DMSO-d_6): δ 7.62 (*d*, 1H, $J = 7.80$ Hz, Ar–**H**), 7.42 (*d*, 1H, $J = 8.00$ Hz, Ar–**H**), 7.24 (*m*, 2H, Ar–**H**), 6.93 (*d*, 2H, $J = 8.40$ Hz, Ar–**H**), 6.70 (*d*, 2H, $J = 8.40$ Hz, Ar–**H**), 5.95 (*t*, 1H, $J = 5.24$ Hz, –CH_2–N**H**– of linker), 4.53 (*d*, 2H, J = 5.28 Hz, –C**H$_2$**–NH– of linker), 4.12 [two overlapped quartets, 4H, (–CH_2–HC–COOC**H**$_2$–CH_3)**$_2$**], 3.84 (*s*, 3H, –C**H$_3$**), 3.55 (*t*, 1H, $J = 7.86$ Hz, –CH_2–**H**C–($COOCH_2$–CH_3)**$_2$**), 2.97 (*d*, 2H, $J = 7.84$ Hz, –C**H$_2$**–CH–($COOCH_2$–CH_3)$_2$), 1.17 [*t*, 6H, $J = 7.20$ Hz –CH_2–CH–($COOCH_2$–C**H$_3$**)**$_2$**]; ^{13}C NMR (100 MHz, DMSO-d_6): δ 168.31 [2C, –CH_2–CH–(**C**OOCH_3)$_2$], 146.83 (C-2), 139 (C-1′), 129.09 (3a and 7a), 125.13 (C-4′), 121.21 (C-3′ and C-5′), 118.58 (C-5 and C-6), 112.32 (C-2′ and C-6′), 109.53 (C-4 and C-7), 60.64 (2C, –CH_2–HC–COO**C**H_2–CH_3)**$_2$**)], 53.45 [-CH_2–H**C**–($COOCH_2CH_3$)$_2$], 40.76 [–**C**H_2–NH– of linker], 33.34 [–**C**H_2–HC–($COOCH_2CH_3$)$_2$], 29.68 [–**C**H_3], 13.76 [2C, –CH_2–HC–($COOCH_2$**C**H_3)**$_2$**]; IR (KBr, cm^{-1}): 3430 (N–H), 2951, 2844, 2866 (C–H), 1641 (C=O);

ESI–MS (m/z) = 409 $[M+1]^+$; anal. calcd. (%) for $C_{23}H_{27}N_3O_4$: C, 67.46; H, 6.65; N, 10.26. Found: C, 68.12; H, 7.01; N, 9.92.

Diethyl(4-{[(1-benzyl-1*H*-benzimidazol-2-yl)methyl]amino} benzyl)malonate (27) Pure product was obtained by column chromatography; yield: 0.081 g, 42.82%; ^{1}H NMR (400 MHz, $CDCl_3$): δ 7.82 (dd, 1H, J = 1.40, 8.24 Hz, Ar–**H**), 7.32 (*m*, 6H, Ar–H), 7.07 (dd, 1H, J = 2.96, 7.52 Hz, Ar–**H**), 7.02 (*d*, 2H, J = 8.48 Hz, Ar–**H**), 6.61 (dd, 2H, J = 2.08, 4.88 Hz, Ar–H), 5.44 (*s*, 2H, benzylic), 4.48 (*s*, 2H, –C**H$_2$**–NH– of linker), 4.53 (*d*, 2H, J = 5.28 Hz, –C**H$_2$**–NH– of linker), 4.18 [two overlapped quartets, 4H, –CH_2–HC–(COOC**H$_2$**–CH_3)**$_2$**], 3.57 (*t*, 1H, J = 4.68 Hz, –CH_2–**H**C–(COOCH_2–CH_3)**$_2$**), 3.10 (*d*, 2H, J = 2.20 Hz, –C**H$_2$**–CH–(COOCH_2–CH_3)$_2$), 1.19 [*t*, 6H, J = 7.28 Hz –CH_2–CH–(COOCH_2–C**H$_3$**)**$_2$**]; IR (KBr, cm^{-1}): 3441 (N–H), 2938 and 2857 (C–H), 1719 (C=O) and 1630 (C=N). ESI–MS (m/z) = 485 $[M]^+$; anal. calcd. (%) for $C_{29}H_{31}N_3O_4$: C, 71.73; H, 6.43; N, 8.65. Found: C, 70.23; H, 6.98; N, 9.12.

Molecular docking methods

Molecular docking in α-glucosidase protein

The crystal structure of the C-terminal domain of human intestinal α-glucosidase protein (PDB code: 3TOP) was used as a molecular target. The crystal structure complex with standard ligand (Acarbose) was downloaded from **RCSB** Protein Data Bank. Water molecules were removed from enzyme structure whereas hydrogens added, energy minimized using Gasteiger–Huckel charges and Tripos force field in the Sybyl software suite. Synthesized compounds were assigned Gasteiger–Huckel charges and subsequently minimized using the Powel method by using SYBYL 7.3 software. The energy-optimized sketched compound was subjected to docking run at the ligand-binding site of α-glucosidase by Surflex dock in SYBYL7.3 (Kaur et al. 2018; Singh et al. 2017, 2018a, b; Mall et al. 2019). Docking analysis was conducted using the Surflex dock module to predict and examine the binding modes of the synthesized derivatives at the active site of α-glucosidase. The hydrogen-bonding interactions (amino acid (AA) residues and bond distances) of the synthesized molecules at the respective active sites were also compared with those of standard drug (Acarbose) (Fig. 3 and Table 1).

Molecular docking in PPARγ protein

The crystal structure of PPARγ (PBD code: 2PRG) complexed with rosiglitazone was selected for the docking study. The protein was energy-optimized, minimized by removing unwanted molecules and other defects reported by the SYBYL 7.3 software (Verma et al. 2013a). All newly synthesized molecules were built onto the crystal structure of rosiglitazone extracted from the crystal structure of PPARγ. They were assigned Gasteiger–Huckel charges and subsequently minimized using the Powel method. The energy-optimized sketched molecules were subjected to docking run at the ligand-binding site of PPARγ by Surflex dock in SYBYL7.3 (Verma et al. 2012a, b, 2013a, b, 2015). Docking analysis was conducted using the Surflex dock module to predict and examine the binding modes of the synthesized derivatives at the active site of PPARγ. The energy-minimized structure of rosiglitazone was initially docked into PPARγ to determine the binding conformation of rosiglitazone at the active sites. The hydrogen-bonding interactions (AA residues and bond distances) of the synthesized molecules at the respective active sites were also compared with those of rosiglitazone (Figs 4, 5 and Table 2).

In vitro assay of α-glucosidase inhibitory activity

For in vitro enzymatic starch digestion method of Granfeldt et al. (1992) was followed with some modifications. One hundred milligram corn starch was put and gelatinized in 3 mL distilled water with or without test compound or Acarbose. To this solution, 4-µg α-amylase was put, vortexed, and the mixture was incubated for 20 min at 80 °C. Then, 3-mL mixture was diluted to 10 mL with distilled water. Then 1 mL of this solution was taken and added to 2 mL of 0.1 M sodium acetate buffer (pH 4.75). To this 3-mL mixture, 30 µg of α-amyloglucosidase was added and the mixture was incubated for 30 min at 60 °C. Samples were removed to the ice to inhibit the thermophilic enzymes. Control samples were having neither Acarbose nor test compound. The inhibitory rate of the test compound on enzymatic starch digestion was calculated by the following equation:

$$(\%)\ \text{inhibition of enzymatic starch digestion} = [A_o - A_i/A_o] \times 100,$$

where A_o = absorbance of the control sample and A_i = absorbance given by test compound.

IC_{50} value (µM) was defined as the amount of test compound reducing the breakdown of starch to glucose by 50% in comparison with the control sample. It was determined by plotting the graph between percentage inhibition of starch digestion verse various concentrations of test compounds (Table 3).

In vitro antioxidant assay

The total radical scavenging capacity of the compounds was determined and compared with standards drug ascorbic acid

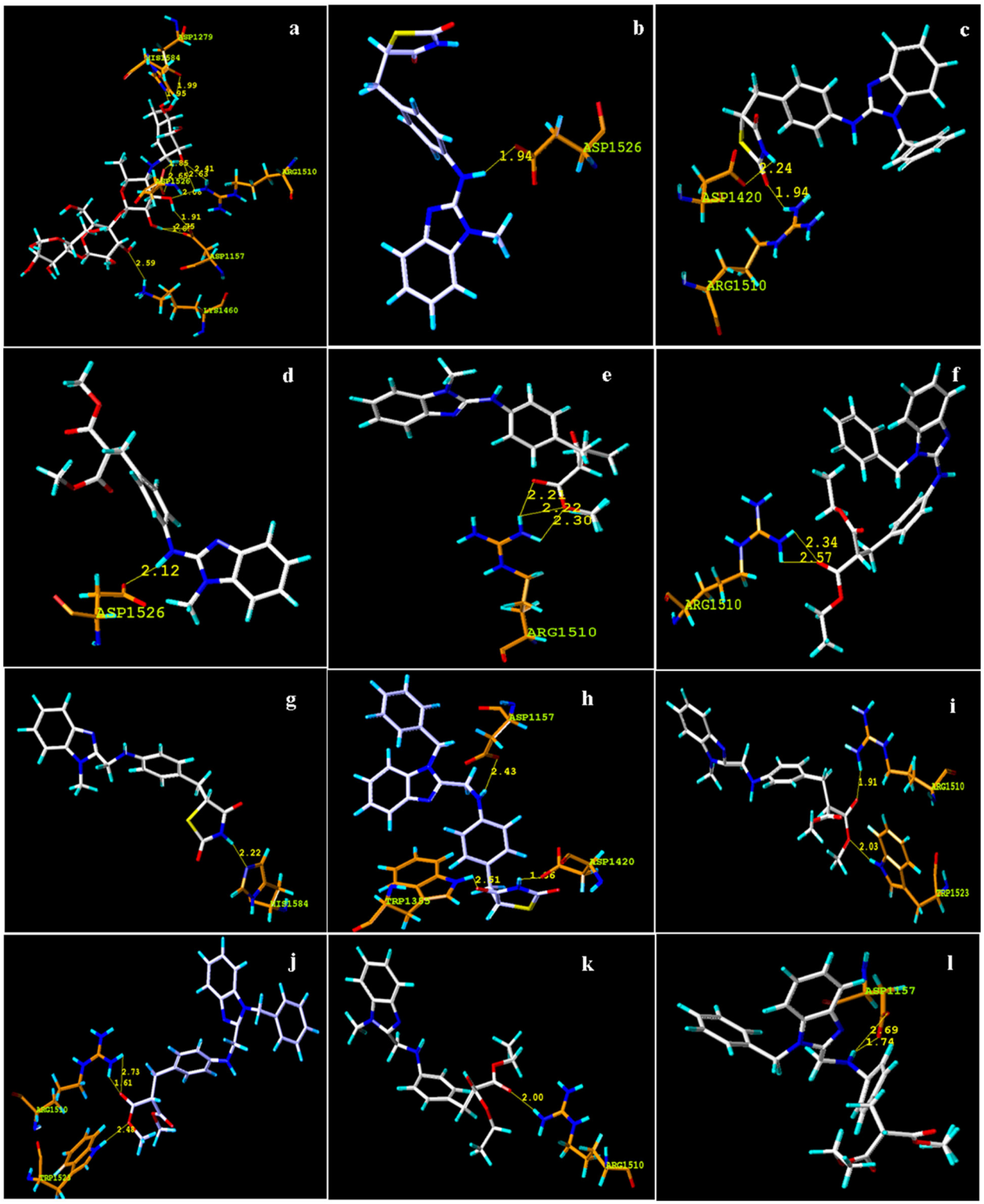

Fig. 3 Molecular interactions of standard drug (Acarbose) and benzimidazole darivatives in the active site of α-glucosidase through hydrogen bonding with potent amino acid residues **a** Acarbose, **b** compound **17**, **c** compound **18**, **d** compound **19**, **e** compound **20**, **f** compound **21**, **g** compound **22**, **h** compound **23**, **i** compound **24**, **j** compound **25**, **k** compound **26**, **l** compound **27**

by using the DPPH (1,1-diphenyl-2-picrylhydrazyl) radical scavenging method and the DPPH radical scavenging activity results of compounds and are summarized in Table 4. One milligram of DPPH was dissolved in 15 ml of methanol (MeOH) and its absorbance was measured at 517 nm. To calculate the percentage scavenging activity different

Table 1 Results of the docking studies of synthesized compounds compared with Acarbose at the active site of α-glucosidase enzyme protein (PDB ID: 3TOP)

Products code	G-score	H-bonding interactions between the ligands and the active site amino acid (AA) residues			
		Atoms of ligands[a]	AA residues	Bond distance (Å)	No. of H-bonds
Acarbose	−160.51	O–**H**	ASP1279	1.99	11
		O–**H**	HIS1584	1.95	
		O–**H**	ASP1526	2.65	
		O–**H**	ASP1526	1.85	
		O–H	ARG1510	2.41	
		O–H	ARG1510	2.63	
		O–H	ARG1510	2.08	
		O–**H**	ASP1157	1.91	
		O–**H**	ASP1157	1.85	
		O–**H**	ASP1157	2.75	
		O–H	LYS1460	2.59	
17	−189.20	N–**H** of linker	ASP1526	1.94	1
18	−216.80	2–C=**O** of TZD	ARG1510	2.24	2
		N–**H** of TZD	ASP1420	1.94	
19	−112.30	N–**H** of linker	ASP1526	2.12	1
20	−125.90	**O**=C–OC_2H_5	ARG1510	2.21	3
		O=C–**O**C_2H_5	ARG1510	2.22	
		O=C–**O**C_2H_5	ARG1510	2.30	
21	−155.60	**O**=C–OC_2H_5	ARG1510	2.34	2
		O=C–OC_2H_5	ARG1510	2.57	
22	−175.23	N–**H** of TZD	HIS1584	2.22	1
23	−212.25	N–**H** of linker	ASP1157	2.43	3
		N–**H** of TZD	ASP1420	1.86	
		4–C=**O** of TZD	TRP1355	2.51	
24	−110.25	**O**=C–OCH_3	ARG1510	1.91	2
		O=C–**O**CH_3	TRP1523	2.03	
25	−115.25	**O**=C–OCH_3	ARG1510	2.73	3
		O=C–OCH_3	ARG1510	1.61	
		O=C–**O**CH_3	TRP1523	2.48	
26	−118.45	**O**=C–OC_2H_5	ARG1510	2.00	1
27	−150.10	N–**H** of linker	ASP1157	2.69	2
		N–**H** of linker	ASP1157	1.74	

[a]The particular atom involved in hydrogen bond formation has been indicated by boldface

concentrations of compounds **17–27** were prepared in MeOH and there were five sets of concentration 0.033, 0.067, 0.100, 0.133, and 0.167 mM for each compound. To evaluate antioxidant activity, 3 mL of the freshly prepared DPPH was added into each set of concentrations and the resulting solution was incubated for 2 h. After incubation, a decrease in absorbance of DPPH was recorded through a UV–visible spectrophotometer at 517 nm. Radical scavenging activity was calculated using the following equation (Arora et al. 2014):

$$(\%)\ \text{Scavenging activity}\ (\%\text{SC}) = [\text{A}_\text{o} - \text{A}/\text{A}_\text{o}] \times 100,$$

where A_o = absorbance at 517 nm due to alone DPPH solution and A = absorbance at 517 nm after adding the antioxidants.

Result and discussion

Chemistry

For the preparation of L.H.S. moieties **3** and **4**, o-phenylenediamine treated with carbon disulfide (CS_2) in the presence of potassium hydroxide (KOH) to give 2-

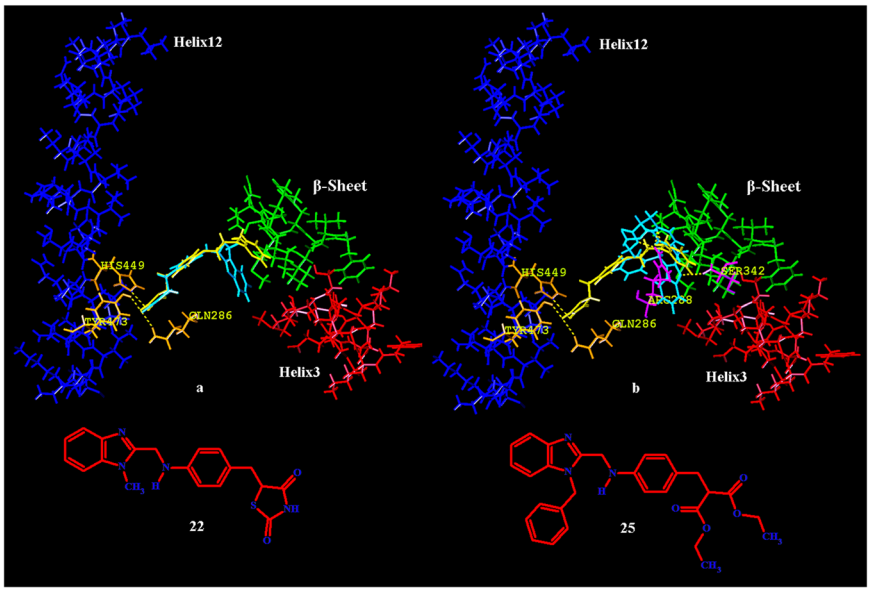

Fig. 4 **a** Crystal structure of rosiglitazone (yellow) (full agonist) interact with H12 of PPARγ ligand-binding domain (LBD) through H-bond with HIS449, TYR473, and GLN286 amino acid residues (orange) and compound **22** (cyan) (full agonist) similarly interact with H12 (blue). **b** Crystal structure of rosiglitazone (yellow), compound **25** (cyan) (partial agonist) interact of PPARγ-LBD through H-bond with SER342 and ARG288 amino acid residue (magenta) and lie between H3 (red) and β-sheet region (green) (Color figure online)

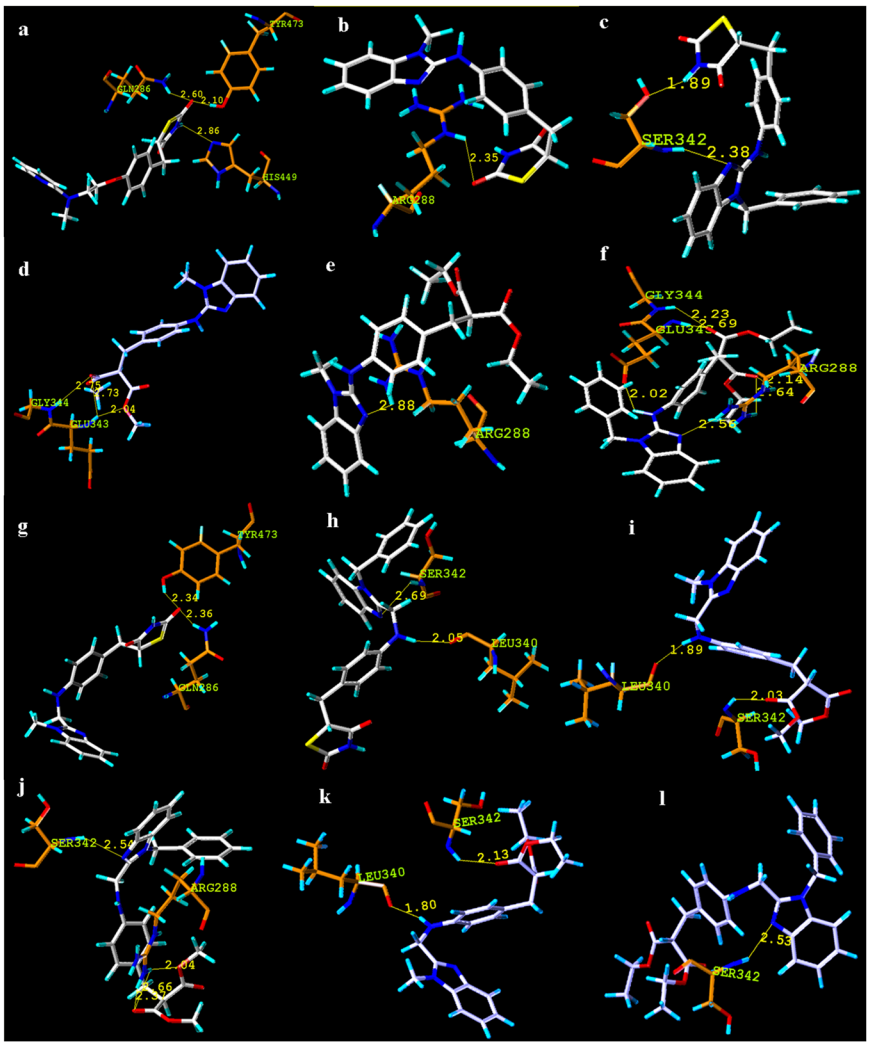

Fig. 5 **a** Crystal structure of rosiglitazone and **b**–**i** of synthesized compounds **17**–**27**, respectively

Table 2 Results of the docking studies of synthesized compounds compared with rosiglitazone at the active site of PPARγ protein (PDB ID: 2PRG)

Compound code	G-score	D score	PMF score	CHEM score	H-bonding interactions between the ligands and the active-site amino acid (AA) residues			
					Atoms of ligands[a]	AA residues	Bond distance (Å)	No. of H-bond
Rosiglitazone	−235.64	−139.26	−61.21	−25.66	2**O**=C of TZD	TYR473	2.10	3
					2**O**=C of TZD	HIS449	2.86	
					3N**H** of TZD	GLN286	2.60	
17	−157.01	−142.12	−45.26	−20.81	2**O**=C of TZD	ARG288	2.35	1
18	−270.20	−161.86	−74.30	−34.32	3-**N** of Benz.	SER342	1.89	2
					N–H of TZD	SER342	2.38	
19	−215.74	−145.98	−49.03	−27.90	O=C–**O**–C_2H_5(a)	GLY344	2.75	3
					O=C–**O**–C_2H_5(a)	GLU343	2.73	
					O=C–**O**–C_2H_5(b)	GLU343	2.04	
20	−181.14	−164.00	−31.97	−21.65	3-**N** of Benz.	ARG288	2.88	1
21	−283.06	−156.67	−26.46	−29.66	3-**N** of Benz	ARG288	2.56	6
					O=C–O–C_2H_5(a)	ARG288	2.64	
					O=C–**O**–C_2H_5(a)	ARG288	2.14	
					N**H** of Linker	GLU343	2.02	
					O=C–O–C_2H_5(b)	GLY344	2.23	
					O=C–**O**–C_2H_5(b)	GLU343	2.69	
22	−245.51	−138.92	−62.50	−29.42	2**O**=C of TZD	TYR473	2.34	2
					2**O**=C of TZD	GLN286	2.36	
23	−340.91	−174.02	−44.16	−40.41	3-**N** of Benz.	SER342	2.69	2
					N**H** of Linker	LEU340	2.05	
24	−220.66	−140.95	−20.74	−33.11	**O**=C–O–CH_3	SER342	2.03	2
					N**H** of Linker	LEU340	1.89	
25	−351.25	−188.94	−4.92	−33.25	3-**N** of Benz.	SER342	2.54	4
					O=C–O–CH_3(a)	ARG288	2.37	
					O=C–O–CH_3(a)	ARG288	2.66	
					O=C–**O**–CH_3(b)	ARG288	2.04	
26	−233.21	−139.45	11.98	−27.19	**O**=C–O–C_2H_5	SER342	2.13	2
					N**H** of Linker	LEU340	1.80	
27	−278.20	−187.28	−24.52	−29.69	3-**N** of Benz.	SER342	2.53	1

[a]The particular atom involved in hydrogen bond formation has been indicated by boldface

mercapto benzimidazole **1** using solvent EtOH, H_2O and glacial acetic acid, which followed by bromination afforded compound 2-bromo benzimidazole **2**, which further treated with dimethyl sulfate and benzyl bromide to yielding 2-bromo-1-methyl-1H-benzimidazole **3** and 1-benzyl-2-bromo-1H-benzimidazole **4** (Scheme 1), respectively.

For the synthesis of **7** and **8**, compound *N*-methylbenzene-1,2-diamine/*N*-benzylbenzene-1,2-diamine **6** treated with chloroacetic acid to afford the desired product (Scheme 2).

The TZD-based R.H.S. moiety **12** was synthesized by reaction Meerwein arylation of 4-Nitroaniline. The diazotization of 4-nitroaniline using $NaNO_2$ and HBr in water/acetone afforded a solution of the corresponding diazonium bromide, which was further condensed with ethyl acrylate using Cu_2O affording ethyl-2-bromo-3-(4-nitrophenyl)propanoate **9**. Cyclization of **9** with thiourea using sodium acetate in hot methanol gave 2-Imino-5-(4-nitrobenzyl)-1,3-thiazolidin-4-one **10** which was followed by hydrolysis with 2 N HCl by refluxing to give 5-(4-nitrobenzyl)-1,3-thiazolidine-2,4-dione **11**, finally, the NO_2 group was reduced with H_2 over Pd/C in methanol to yield R.H.S. moiety 5-(4-aminobenzyl)-1,3-thiazolidine-2,4-dione **12** (Scheme 3). Two RHS intermediate moieties i.e., dimethyl(4-aminobenzyl)malonate **15** and diethyl(4-aminobenzyl)malonate **16** were synthesized in two steps (Scheme 4). First, 4-

nitrobenzaldehyde condensed with dimethyl malonate/diethyl malonate by Knoevenagel condensation using piperidinium acetate as base and toluene as solvent under reflux condition to give dimethyl(4-nitrobenzylidene)malonate **13**/diethyl(4-nitrobenzylidene)malonate **14** which on further NO_2 groups were reduced by catalytic hydrogenation with 10% palladium on carbon to get desired RHS moieties **15** and **16**. The coupling of L.H.S. with R.H.S. intermediates to afford all targeted molecules **17–27** under the microwave condition using MeOH as solvent (Schemes 5 and 6).

In the NMR spectra of TZD-based targeted compounds with –NH– linker **17/18**, the appearance of –NH– linker protons 1H singlet at δ (ppm) 10.68/10.78 along with the presence of peaks at *m/z* 353 $[M+1]^+$ and 428 $[M]^+$ in the mass spectrum of **17** and **18**, respectively, provides an additional support to the structure assigned to these molecules (Scheme 5).

Table 3 In vitro α-glucosidase inhibitory activity of the synthesized compounds in comparison with Acarbose (Standard Drug)

Compounds	α-glucosidase IC_{50} (μM)
17	8.70 ± 0.06
18	4.10 ± 0.01
19	31.5 ± 1.01
20	22.50 ± 0.70
21	15.60 ± 0.60
22	9.12 ± 0.06
23	4.50 ± 0.02
24	32.50 ± 1.02
25	29.02 ± 0.85
26	25.02 ± 0.07
27	16.80 ± 0.75
Acarbose	15.4 ± 0.63

It was found in the NMR spectra of other two TZD-based targeted compounds with $–CH_2NH–$ linker **22/23**, the appearance of $–CH_2N\mathbf{H}–$ linker protons 1H triplet at δ (ppm) 6.06/6.15 along with the presence of 2H doublets for $–C\mathbf{H}_2NH–$ linker at δ (ppm) 4.52/4.49 along with the presence of peaks at *m/z* 367 $[M+1]^+$ and 443 $[M+1]^+$ in the mass spectrum of **22** and **23**, respectively, provides an additional support to the structure assigned to these molecules. Moreover, N–H stretching bands at 3428 and 3422 present in molecules **22** and **23**, respectively, confirm the coupling of appropriate L.H.S. and R.H.S. to get desired compounds (Scheme 6).

The DMM-based compound **19** was confirmed by the appearance of broad 1H singlet at δ (ppm) 12.98 due to –N**H**– of the linker in the NMR spectrum. In the FTIR spectrum, N–H stretching band appeared at 3377 cm^{-1} along with C=O stretch at 1732 cm^{-1} confirmed the structure assigned. The presence of a peak at *m/z* 367 $[M]^+$ in the mass spectrum of **19** provides additional support to the structure assigned to this molecule.

The characteristic signals for $–CH_2N\mathbf{H}–$ linker proton 1H triplet at δ (ppm) 6.04 along with 2H doublets for $–C\mathbf{H}_2NH–$ linker at δ (ppm) 4.52 appeared in the NMR spectrum of DMM-based compound **24**. The **N–H** and stretching bands at 3402 and 1647 cm^{-1} were recorded in the FTIR spectrum and the presence of $[M+1]^+$ peak at *m/z* 382 in the mass spectrum of compound **24** provided additional support to structure assigned for this compound.

Another DMM-based compound **25** was confirmed by the appearance of characteristic signals for $–CH_2N\mathbf{H}–$ linker protons 1H dd at δ (ppm) 7.81 along with the presence of 2H singlet for $–C\mathbf{H}_2NH–$ linker at δ (ppm) 4.45 in NMR spectrum along with N–H and C=O stretching bands at 3441 and 1726, respectively, in FTIR spectrum. The presence of $[M]^+$ peak at *m/z* 457 in the mass spectrum of compound **25** provided additional support to the structure assigned for this compound.

Table 4 Evaluation of in vitro antioxidant activity (DPPH assay)

Compounds	Percentage (%) antioxidant activity at concentration (mM/L)					EC_{50} (mM)
	0.033 mM	0.067 mM	0.100 Mm	0.133 mM	0.167 mM	
17	4.87 ± 2.1	23.49 ± 0.6	32.76 ± 0.6	36.45 ± 0.7	41.02 ± 0.7	0.189 ± 0.005
18	6.53 ± 1.1	25.31 ± 0.8	33.57 ± 1.0	38.40 ± 0.6	44.38 ± 0.7	0.176 ± 0.002
19	0.88 ± 0.1	2.14 ± 0.5	7.35 ± 0.7	12.32 ± 0.6	20.20 ± 0.8	0.383 ± 0.008
20	9.17 ± 0.8	13.26 ± 0.8	18.31 ± 0.7	22.40 ± 0.3	25.23 ± 0.7	0.364 ± 0.009
21	10.43 ± 0.6	15.60 ± 0.4	19.33 ± 0.5	23.40 ± 0.4	26.37 ± 0.5	0.361 ± 0.017
22	7.48 ± 1.2	20.49 ± 0.9	33.50 ± 1.5	38.29 ± 0.6	40.67 ± 0.4	0.186 ± 0.002
23	7.69 ± 1.1	22.53 ± 0.9	33.42 ± 0.8	36.41 ± 0.9	42.30 ± 0.7	0.186 ± 0.002
24	4.29 ± 0.7	9.04 ± 1.4	11.82 ± 1.1	15.26 ± 0.8	21.64 ± 2.4	0.408 ± 0.030
25	6.12 ± 0.8	9.77 ± 1.5	12.43 ± 0.7	16.49 ± 0.9	23.72 ± 1.8	0.395 ± 0.030
26	7.52 ± 0.7	10.26 ± 0.7	14.39 ± 0.7	18.37 ± 0.8	23.17 ± 0.7	0.399 ± 0.026
27	7.16 ± 0.8	10.76 ± 0.4	17.50 ± 0.6	21.18 ± 1.0	26.48 ± 1.0	0.323 ± 0.011
Ascorbic acid	14.39 ± 0.6	30.45 ± 0.7	41.66 ± 0.3	57.13 ± 0.6	73.11 ± 0.9	0.115 ± 0.000

Scheme 1 Reagents and conditions: **a** carbon disulfide, EtOH, H_2O, glacial acetic acid; **b** HBr/glacial acetic acid, Br_2, H_2O, NaOH; **c** $(CH_3)_2SO_4$, 1 N NaOH; **d** benzyl bromide, NaH/dry DMF

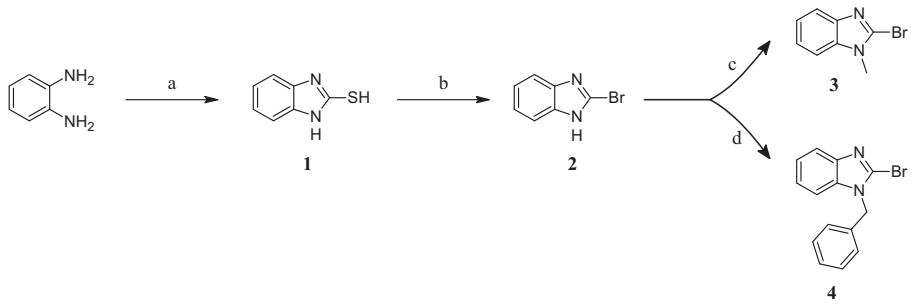

Scheme 2 Reagents and conditions: **a** benzyl bromide, H_2O, reflux, 4 h; **b** $SnCl_2{\cdot}2H_2O$, EtOH, reflux, 2 h; **c** chloroacetic acid, 4 N HCl, EtOH, reflux, 3 h

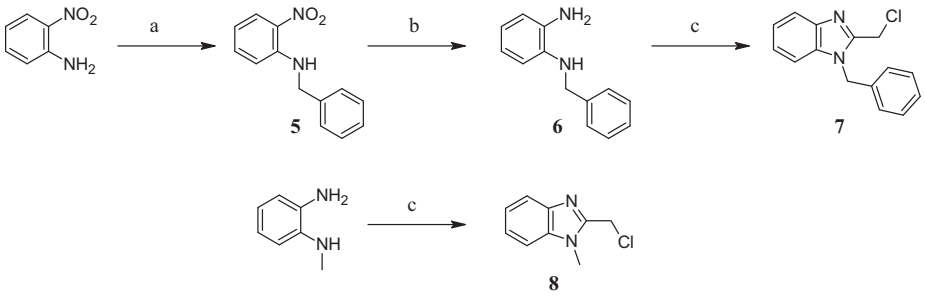

Scheme 3 Reagents and conditions: **a** $NaNO_2$, HBr, H_2O, acetone, MeOH, ethyl acrylate, Cu_2O; **b** thiourea, sodium acetate, MeOH; **c** 2 N HCl; **d** Pd–C, H_2, MeOH

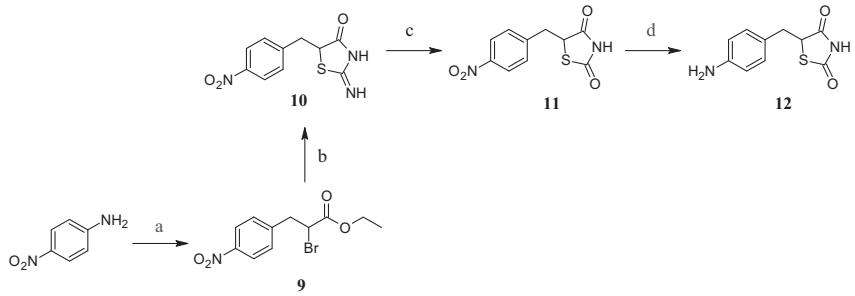

Scheme 4 Reagents and conditions: **a** piperidinium acetate, toluene; **b** Pd–C, H_2, MeOH

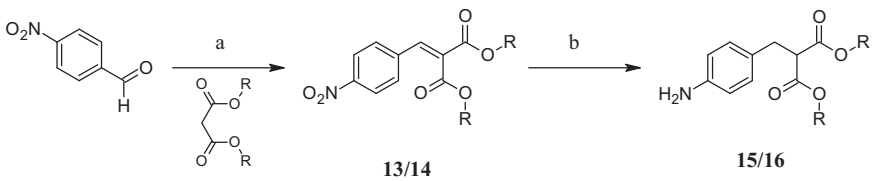

Code	R
13, **15**	Me
14, **16**	Et

The DEM-based compound **20** was confirmed by the appearance of –N**H**– linker protons 1H singlet at δ (ppm) 13.04 in the NMR spectrum along with N–H and C=O stretching bands at 3438 and 1738 cm^{-1} in FTIR spectrum. Further, the structure was also confirmed by the presence of $[M]^+$ peak at *m/z* 395 in the mass spectrum of compound **20**.

The N–H and C=O stretching bands at 3432 and 1639 cm^{-1} were recorded in the FTIR spectrum of compound **21**. The NMR spectrum also indicated the formation of the product by containing 13 aromatic protons along with the appearance of two overlapped quartets due to 4H at δ (ppm) 4.14, one triplet at δ 1.21 due to 6H of DEM part of the compound. The presence of $[M+1]^+$ peak at *m/z* 472 in the mass spectrum of compound **21** also confirmed the structure.

In the NMR spectra of other two DEM-based targeted compounds with –CH_2NH– linker **26/27**, the appearance of

Scheme 5 Reagent and condition: **a** EtOH, microwave, 15 min

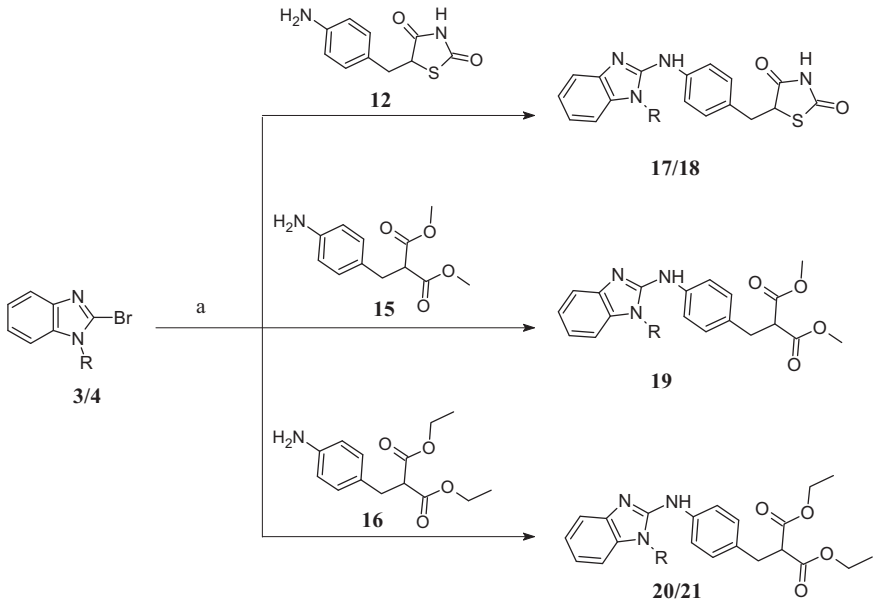

Codes	R
3, **17**, **19**, **20**	Me
4, **18**, **21**	Bn

Scheme 6 Reagent and condition: **a** EtOH, microwave, 15 min

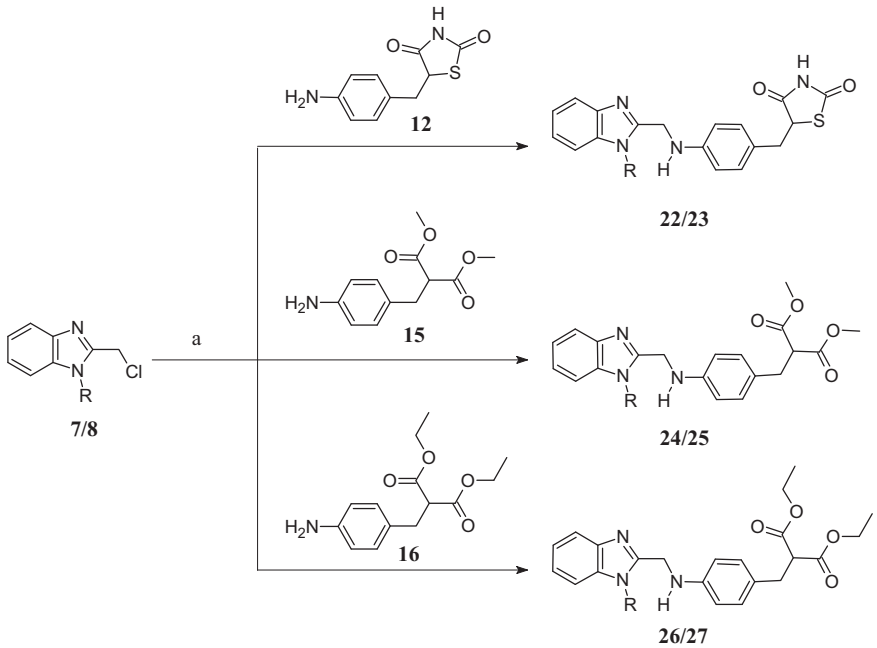

Codes	R
7, **22**, **24**, **26**	Me
8, **23**, **25**, **27**	Bn

–CH_2N**H**– linker protons 1H triplet at δ (ppm) 5.95/4.48 along with the presence of 2H doublets for –C**H**$_2$NH– linker at δ (ppm) 4.53/4.48, respectively, confirms coupling of appropriate L.H.S. and R.H.S. to get desired compounds through microwave-assisted synthesis. The appearance of bands corresponding to N–H at 3430 and 3441 cm^{-1} along

with C=O stretch at 1641 and 1719 cm^{-1} for compounds **26** and **27**, respectively, in the FTIR spectra confirmed the structures of compounds. The presence of peaks at *m/z* 409 $[M+1]^+$/485 $[M]^+$ in the mass spectrum of compound **26/27**, respectively, provided the additional support to structures assigned.

Molecular docking

Molecular docking in α-glucosidase protein (PDB ID: 3TOP)

All the final synthesized compounds **17–27** were docked (with Surflex dock module of Sybyl 7.3, Tripose Inc. software available at our in silico drug design Laboratory) at the binding site of C-terminal domain of human intestinal α-glucosidase (PDB Code: 3TOP) for the prediction of binding affinities in terms of Gold score energies (G-score) and H-bond interactions in comparison with reference to the standard molecule (Acarbose) (Yousefi et al. 2015; Kaur et al. 2018; Singh et al. 2017, 2018a, b; Mall et al. 2019). It was found from the analysis of docking results that the binding affinity of Acarbose in terms of G-score is −160.51 and it binds through hydrogen bonds formation with ASP1526, ASP1279, ASP1157, HIS1584, ARG1510, and LYS1460 AA residues. The comparison of the predicted binding affinities in terms of G-score of the synthesized ligands with that of Acarbose showed that all synthesized compounds **17** (−189.20), **18** (−216.80), **22** (−175.23), **23** (−212.25) with TZD group have higher binding affinities than that of Acarbose but DMM-based compounds **19** (−112.30), **24** (−110.25), **25** (−115.25), and DEM-based compounds **20** (−125.90), **21** (−155.60), **26** (−118.45) and **27** (−150.10) have lower binding affinities than that of Acarbose (Table 1). Detailed analysis of H-bonding interactions showed that all NCEs interacted with at least one AA residue, which was interacting with Acarbose so it is expected that all NCEs are known to possess α-glucosidase inhibitory activities. The H-bonding interactions between the final compounds (**17–27**) and the AA residues in the active sites of protein (PDB code: 3TOP) were explored and compared with those of Acarbose to explain the binding modes and binding affinities of the ligands. The TZD-based compound **17** formed H-bond with ASP1526 through –N**H**– of a linker, compound **18** interacted through acidic parts –N**H**– and C=**O** of TZD ring with AA residue ASP1420 and ARG1510, respectively, compound **22** interacted with HIS1584 AA residue through acidic H of –N**H**– of TZD group whereas compound **23** interacted through acidic H –N**H**– of the linker, N**H** and C=**O** of TZD ring with ASP1157, ASP1420, TRP1355 respectively. The DMM-based compound **19** formed H-bond with ASP1526 through acidic H of –N**H**– of the linker, compound **24** interacted with AA residues ARG1510 and TRP1523 through **O**=C of **O**=C–OCH_3 and O=C–OCH_3 part of ester group, respectively, and similarly compound **25** interacted with two ARG1510 AA residues through **O**=C–OCH_3 and TRP1523 through O=C–**O**CH_3 part of the ester group. The DEM-based compound **20** formed three H-bond with ARG1510 through one **O**=C–OC_2H_5 and two O=C–**O**C_2H_5 part of ester group whereas compound **21** interacted through **O**=C–OC_2H_5 with two ARG1510 AA residues, compound **26** also formed H-bond with ARG1510 AA residues through **O**=C–OC_2H_5 whereas compound **27** interacted through –N**H**– of the linker with two ASP1157 (Fig. 3). Molecular docking studies were found to be under that of in vitro studies.

Molecular docking in PPARγ protein (PDB ID 2PRG)

The NCEs (**17–27**) were docked into the binding site of PPARγ protein (PDB Code: 2PRG) by taking rosiglitazone as a reference molecule. The output of these docking studies corresponds to the prediction of binding affinities in terms of G-score, and hydrogen-bonding interactions of all the synthesized compounds with AA residues in the active site of PPARγ protein are shown in Table 2. The hydrogen (H)-bonding of rosiglitazone and synthesized compounds (**17–27**) with AA residues of the PPARγ protein and their H-bond distances are shown in Fig. 4. The comparison of the predicted binding affinities in terms of GOLD-scores or G-scores of the synthesized compounds with that of rosiglitazone showed that compounds **18** (−270.20), **21** (−283.06), **22** (−245.51), **23** (−340.91), **25** (−351.25), and **27** (−278.20) have higher G-scores corresponding to higher binding affinity in the active site of PPARγ protein. On the other hand compound **19** (−215.74), **24** (−220.66), and **26** (−233.21) have comparable G-scores with rosiglitazone (−235.64) showed good binding affinity whereas compounds **17** (−157.01) and **20** (−181.14) have bit lesser binding affinity. It was reported in the literature and here we also found that when rosiglitazone was docked in PPARγ protein, the TZD moiety of rosiglitazone enters into H-bonding interaction with GLN286, HIS449, and TYR473 AA residue (Table 2 and Fig. 5a). TYR473 AA in the ligand-binding domain of Helix12 (H12) is a critical site of interaction between the "full agonist" and the PPARγ receptor which is responsible for the undesirable side effects (Liu et al. 2011). PPARγ partial agonists cause activation and stabilization of PPARγ by interacting with AA of β-sheet and Helix3 (H3) (Bruning et al. 2007; Einstein et al. 2008), which is distinct as compared with full agonists (stabilizer of AAs of H12). Only one compound **22** out of eleven synthesized compounds showed interaction with TYR473 AA residue through the C=O group at the second position of TZD ring to act as PPARγ full agonists similarly as showed by Rosiglitazone. Rest of the compounds **17**, **18**,

19, **20**, **21**, **23**, **24**, **25**, **26**, and **27** interacted with important SER342 and ARG288 AA residue of β-sheet through H-bonding which act as partial agonists in the PPARγ protein. The SAR of these synthesized compounds has been established. The results showed that linkers play an important role in the orientation of compounds into the active site of the protein. The molecules (**21**–**27**) having –CH_2–NH– linker (two atoms linker) interacted with SER342 AA residue of β-sheet except one compound **22**, which interacted with TYR473 AA of Helix12. On the other hand, out of five compounds **17**–**21** with –NH– linker (one atom liker) only one compound **18** interacted with SER342 AA, four compounds **17** and **19**–**21** formed the H-bond with ARG288, GLU343, and GLY344 AA residue of β-sheet. It was also observed that the compounds containing benzyl group at 1-position of benzimidazole showed higher G-score value than their respective methyl-containing compounds. The structural features observed in these two series with –NH– and –CH_2–NH– linkers for the active nature of compounds are the presence of hydrogen-bonding parts (TZD, DMM, and DEM) and heterocyclic parts (*N*-alkyl benzimidazole). Among linkers, –CH_2–NH– linker-containing compounds were found superior to –NH– linker, and *N*-benzyl-substituted compounds were found superior to *N*-methyl-substituted compounds in this study. The compounds contain TZD group **17**, **18**, and **23** interact with AA of β-sheet and H3 i.e., SER342 and ARG288 to act as PPARγ partial agonist except compound **22** containing methyl group interact with TYR473 and GLN286 AA of H12 to act as a full agonist. Compound **23** with a benzyl substitution at the 1-position of benzimidazole and a TZD group at the 4-position of the phenyl ring with –CH_2NH– linker has the highest G-score = −340.91 as well as interacted with SER342, and LEU340 AA residue was found to be the most active partial agonist. Compounds **19**, **24**, and **25** contain DMM instead of TZD as hydrogen-bonding part. Compound **19** interact with AA GLY344 and GLU343, compound **24** with SER342, LEU340 AA residue, and **25** with SER342 and ARG288, which belongs to β-sheet and H3 to act as partial agonists. DEM-based compounds **20, 21, 26**, and **27** formed the H-bonds with AA residues of β-sheet and H3 i.e., ARG288, GLU343, GLY344, LEU340, and SER342 to act as partial agonists. The results showed that compounds containing benzyl group at 1-position of benzimidazole interacted with AA residues of β-sheet and H3 to act as partial agonists. This may be because of the presence of a large phenyl group instead of a methyl group to support fit into the cavity of PPARγ protein to interact with AA residues of β-sheet and H3.

α-Glucosidase inhibitory activity

All targeted compounds (**17**–**27**) were evaluated for their in vitro α-glucosidase inhibitory activity using Acarbose as a positive control ($IC_{50} = 15.4 \pm 0.63$ μM) (Table 3). All tested compounds showed potent α-glucosidase inhibitory activity with IC_{50} ranging from $IC_{50} = 4.10 \pm 0.01$ to $IC_{50} = 31.5 \pm 1.01$ μM, in comparison with standard drug Acarbose ($IC_{50} = 15.4 \pm 0.63$ μM). It was revealed from biological studies that the presence of linkers (**–NH–** and **–CH_2NH–**) and H-bonding parts (i.e., TZD, DMM, and DEM) both play an effective role in this assay. It has been revealed from the biological results that *N*-benzylbenzimizazolyl-based compounds (**18, 21, 23, 25**, and **27**) have a better inhibitory effect than corresponding *N*-methylbenzimizazolyl-based compounds (**17, 19, 20, 22, 24**, and **26**).

It has also been concluded from biological results that TZD-based compounds **17** ($IC_{50} = 8.70 \pm 0.06$ μM)**, 18** ($IC_{50} = 4.10 \pm 0.01$ μM)**, 22** ($IC_{50} = 9.12 \pm 0.06$ μM), and **23** ($IC_{50} = 4.50 \pm 0.02$ μM) have better inhibition than standard drug ($IC_{50} = 15.40 \pm 0.63$ μM). Further out of the four compounds, two compounds **18** and **23** with *N*-benzyl benzimidazolyl-based compounds have more inhibition potential. All the DMM- and DEM-based compounds **19** ($IC_{50} = 31.5 \pm 1.01$ μM), **20** ($IC_{50} = 22.50 \pm 0.70$ μM), **21** ($IC_{50} = 15.60 \pm 0.60$ μM), **24** ($IC_{50} = 32.50 \pm 1.02$ μM), **25** ($IC_{50} = 29.02 \pm 0.85$ μM), **26** ($IC_{50} = 25.02 \pm 0.07$ μM), and **27** ($IC_{50} = 16.80 \pm 0.75$ μM) compounds showed lesser inhibition potential than Acarbose ($IC_{50} = 15.40 \pm 0.63$ μM). The substitution of nitrogen of benzimidazole with the bulkier benzyl group increases the inhibitory activity. The binding interactions of targeted compounds **(17–27)** were proved through molecular docking studies. Molecular docking studies in terms of G-score values and binding interaction of novel-targeted compounds in comparison with the standard drug (Acarbose) in the active site of the enzyme has also supported the biological activity studies. Overall a significant correlation was found between the docking studies and α-glucosidase inhibition of active compounds by displaying a good correlation coefficient ($r^2 = 0.9476$) between G-score and IC_{50} values. The correlation curve and the value of the correlation coefficient are given in (Fig. 6).

The SAR of these compounds has been established. The result suggested that the targeted compounds (**17, 18, 22**, and **23**) with the thiazolidine-2,4-dione group located at 4-position of the phenyl ring showed the best activity. Replacement of thiazolidine-2,4-dione with dimethyl malonate and diethyl malonate groups (**19, 20, 21, 24, 25, 26 and 27**), which are acyclic analogs of isoxazolidienedione i.e., further cyclic analogs of TZD, decreases the activity drastically (Table 3).

Antioxidant activity

The DPPH radical model is the most commonly used method for rapid evaluation of the free radical scavenging

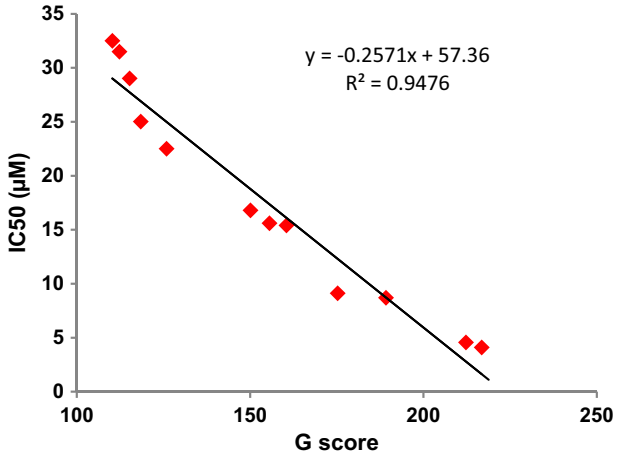

Fig. 6 Correlation between IC_{50} and docking score values of compounds

activity of organic compounds. Synthesized compounds **17**–**27** were evaluated for their antioxidant potential and compared with standard ascorbic acid (Table 4).

Among the series, TZD-based compounds **17** (EC50 = 0.189 ± 0.005 mM), **18** (EC50 = 0.176 ± 0.002 mM), **22** (EC50 = 0.186 ± 0.002 mM), and **23** (EC50 = 0.186 ± 0.002 mM) showed comparable potent antioxidant activity to standard ascorbic acid (EC50 = 0.115 ± 0.000 mM). In particular, compound **18** (EC50 = 0.176 ± 0.002 mM) with a benzyl substitution at the 1-position of benzimidazole and a TZD group at the 4-position of the phenyl ring with –NH– linker was found to be the most active compound. Although in the literature, three different mechanisms could be regarded for the deactivation of free radicals (Ozil et al. 2016c; Najafi et al. 2012; Musialik and Litwinienko 2005; Musialik et al. 2009). Taking into account hydrogen-donating capability of antioxidant, the TZD-based compounds (**17**, **18**, **22**, **23**) are considered better than DMM-based **19** (EC50 = 0.383 ± 0.008), **24** (EC50 = 0.408 ± 0.030), **25** (EC50 = 0.395 ± 0.030) and DEM-based compounds **20** (EC50 = 0.364 ± 0.009), **21** (EC50 = 0.361 ± 0.017), **26** (EC50 = 0.399 ± 0.026), **27** (EC50 = 0.323 ± 0.011) because of more number of labile hydrogen. Further it has also been observed that benzyl substituted at 1-position of benzimidazole derivatives **18**, **21**, **23**, **25**, and **27** have higher antioxidant activity than their respective methyl-substituted compounds **17**, **19**, **20**, **22**, and **24** (Ozil et al. 2016c).

Conclusions

A novel series of compounds (**17**–**27**) synthesized through microwave-assisted reactions. All synthesized compounds (**17**–**27**) docked in the active site of α-glucosidase protein (PDB ID: 3TOP) and evaluated for their inhibitory action against α-glucosidase. Comparative evaluation of these compounds revealed that compound **18** showed maximum inhibitory potential against α-glucosidase giving an IC_{50} of 4.10 ± 0.01 μM. The compounds (**17, 18, 22**, and **23**) were more inhibitive to these enzymes than the rest of the tested compounds with IC_{50} values of much lower than that of the positive control (Acarbose, Standard Drug). The results of molecular docking studies have also supported the in vitro studies. All synthesized compounds (**17**–**27**) also evaluated for their antioxidant potential. Compound **18** with EC_{50} = 0.176 ± 0.002 mM came up with the most potent results, which turn out inhibition against DPPH using ascorbic acid as the reference drug.

On the other hand, all synthesized compounds (**17**–**27**) docked in the active site of PPARγ protein (PDB ID: 2PRG). It was found from the analysis of docking results at the active site of PPARγ protein that compound **23** has highest G-score = −340.91 as well as interacted with SER342, and LEU340 AA residue of β-sheet was found to be the best PPARγ partial agonist (Fig. 4b). Similar interaction with SER342 is also shown by compounds **18** and **24**–**27**, and have the desired potential to act as PPARγ partial agonists. Compound **22** on the other hand interacted with TYR473 and GLN286 AA of H12, almost similar to that of rosiglitazone (standard drug) and has the potential to act as a PPARγ full agonist (Fig. 4a).

Acknowledgements Authors are thankful to the Punjabi University, Patiala authorities for providing the necessary research facilities. We are also grateful to Director and Mr Avtar Singh of Sophisticated Analytical Instrumentation Facility (SAIF), Panjab University, Chandigarh, respectively, for extending the facilities for spectral analysis of the compounds reported in this paper. One of the authors, GS, is thankful to the Ministry of Social Justice and Empowerment, Govt of India for providing research fellowship.

Compliance with ethical standards

Conflict of interest The authors declare that they have no conflict of interest.

Publisher's note Springer Nature remains neutral with regard to jurisdictional claims in published maps and institutional affiliations.

References

Akhtar W, Khan MF, Verma G, Shaquiquzzaman M, Rizvi MA, Mehdi SH, Akhter M, Alam MM (2017) Therapeutic evolution of benzimidazole derivatives in the last quinquennial period. Eur J Med Chem 126:705–753

Albrecht SS, Kuklina EV, Bansil P, Jamieson DJ, Whiteman MK, Kourtis AP, Posner SF, Callaghan WM (2010) Diabetes trends among delivery hospitalizations in the U.S., 1994–2004. Diabetes Care 33:768–773

Arora RK, Kaur N, Bansal Y (2014) Novel coumarin–benzimidazole derivatives as antioxidants and safer anti-inflammatory agents. Acta Pharm Sin B 4:368–375

Arshad T, Khan KM, Rasool N, Salar U, Hussain S, Tahir T, Ashraf M, Wadood A, Riaz M, Perveen S, Taha M, Ismail NH (2016) Syntheses, in vitro evaluation and molecular docking studies of 5-bromo-2-aryl benzimidazoles as α-glucosidase inhibitors. Med Chem Res 25:2058–2069

Berger J, Moller DE (2002) The mechanisms of action of PPARs. Annu Rev Med 53:409–435

Bruning JB, Chalmers MJ, Prasad S, Busby SA, Kamenecka TM, He Y, Nettles KW, Griffin PR (2007) Partial agonists activate PPARγ using a helix 12 independent mechanism. Structure 15:1258–1271

Carmona MC, Louche K, Lefebvre B, Pilon A, Hennuyer N, Bouchez VA, Fievet C, Torpier G, Formstecher P, Renard P, Lefebvre P, Dacquet C, Staels B, Casteilla L, Penicaud L (2007) S 26948: a new specific peroxisome proliferator–activated receptor modulator with potent antidiabetes and antiatherogenic effects. Diabetes 56:2797–2808

Ceriell A (2000) Oxidative stress and glycemic regulation. Metabolism 49:27–29

Chakrabarti R, Rajagopalan R (2002) Diabetes and insulin resistance associated disorders: disease and the therapy. Curr Sci 83:1533–1538

Chinthala Y, Domatti AK, Sarfaraz A, Singh SP, Arigari NK, Gupta N, Satya SKVN, Kumar JK, Khan F, Tiwari AK, Paramjit G (2013) Synthesis, biological evaluation and molecular modeling studies of some novel thiazolidinediones with triazole ring. Eur J Med Chem 70:308–314

Dhameja M, Gupta P (2019) Synthetic heterocyclic candidates as promising α-glucosidase inhibitors: an overview. Eur J Med Chem 176:343–377

Dinparast L, Valizadeh H, Bahadori MB, Soltani S, Asghari B, Rashidi MR (2016) Design, synthesis, α-glucosidase inhibitory activity, molecular docking and QSAR studies of benzimidazole derivatives. J Mol Struct 1114:84–94

Einstein M, Akiyama TE, Castriota GA, Wang CF, McKeever B, Mosley RT, Becker JW, Moller DE, Meinke PT, Wood HB, Berger JP (2008) The differential interactions of peroxisome proliferatoractivated receptor ligands with TYR473 is a physical basis for their unique biological activities. Mol Pharm 73:62–74

Ghani U (2015) Re-exploring promising α-glucosidase inhibitors for potential development into oral anti-diabetic drugs: Finding needle in the haystack. Eur J Med Chem 103:133–162

Granfeldt Y, Björck I, Drews A, Tovar J (1992) An in vitro procedure based on chewing to predict metabolic response to starch in cereal and legume products. Eur J Clin Nutr 46:649–660

Gray GM (1975) Carbohydrate digestion and absorption—role of the small intestine. N Eng J Med 292:1225–1230

Guasch L, Sala E, Valls C, Blay M, Mulero M, Arola L, Pujadas G, Vallvee SG (2011) Structural insights for the design of new PPARgamma partial agonists with high binding affinity and low transactivation activity. J Comput Aided Mol Des 25:717–728

Hirose H, Yamasaki T, Ogino M, Mizojiri R, Tamura OY, Yashiro H, Muraki Y, Nakano Y, Sugama J, Hata A, Iwasaki S, Watanabe M, Maekawa T, Kasai S (2017) Discovery of novel 5-oxa-2,6-diazaspiro[3.4]oct-6-ene derivatives as potent, selective, and orally available somatostatin receptor subtype 5(SSTR5) antagonists for treatment of type 2 diabetes mellitus. Bioorg Med Chem 25:4175–4193

Ibrahim MK, Eissa IH, Abdallah AE, Metwaly AM, Radwan MM, ElSohly MA (2017) Design, synthesis, molecular modeling and anti-hyperglycemic evaluation of novel quinoxaline derivatives as potential PPARγ and SUR agonists. Bioorg Med Chem 25:1496–1513

Kaku K (2014) Efficacy of voglibose in type 2 diabetes. Expert Opin Pharm 15:1181–1190

Kaur J, Singh A, Singh G, Verma RK, Mall R (2018) Novel indolyl linked *para*-substituted benzylidene-based phenyl containing thiazolidienediones and their analogs as α-glucosidase inhibitors: synthesis, in vitro, and molecular docking studies. Med Chem Res 27:903–914

Kim T, Choi HJ, Eom SH, Lee J, Kim TH (2014) Potential α-glucosidase inhibitors from thermal transformation of (±)-catechin. Bioorg Med Chem Lett 24:1621–1624

Liu W, Lau F, Liu K, Wood HB, Zhou G, Chen Y, Li Y, Akiyama TE, Castriota G, Einstein M, Wang C, McCann ME, Doebber TW, Wu M, Chang CH, McNamara L, McKeever B, Mosley RT, Berger JP, Meinke PT (2011) Benzimidazolones: a new class of selective peroxisome proliferator activated receptor γ (PPARγ) modulators. J Med Chem 53:8541–8554

Mall R, Singh A, Singh G, Singh V, Verma RK (2019) Indolyl linked *meta*-substituted benzylidenes as novel ligands: synthesis, biological evaluation, and molecular docking studies. J Heterocycl Chem 56:1542–1555

Mavrova AT, Yancheva D, Anastassova N, Anichina K, Zvezdanovic J, Djordjevic A, Markovic D, Smelcerovic A (2015) Synthesis, electronic properties, antioxidant and antibacterial activity of some new benzimidazoles. Bioorg Med Chem 23:6317–6326

Menteşe E, Ulker S, Kahveci B (2015) Synthesis and study of α-glucosidase inhibitory, antimicrobial and antioxidant activities of some benzimidazole derivatives containing triazole, thiadiazole, oxadiazole, and morpholine rings. Chem Heterocycl Compd 5:1671–1685

Mizuno CS, Chittiboyina AG, Kurtz TW, Pershadsingh HA, Avery MA (2008) Type 2 diabetes and oral antihyperglycemic drugs. Curr Med Chem 15:61–74

Musialik M, Kuzmicz R, Pawłowski TS, Litwinienko G (2009) Acidity of hydroxyl groups: an overlooked influence on antiradical properties of flavonoids. J Org Chem 74:2699–2709

Musialik M, Litwinienko G (2005) Scavenging of dpph$^{\bullet}$ radicals by vitamin E is accelerated by its partial ionization: the role of sequential proton loss electron transfer. Org Lett 7:4951–4954

Najafi M, Najafi M, Najafi H (2012) DFT/B3LYP study to investigate the possible ways for the synthesize of antioxidants with high efficiency based on vitamin E. Bull Korean Chem Soc 33:3343–3348

Notkins AL (2002) Immunologic and genetic factors in Type 1 diabetes. J Biol Chem 277:43545–43548

Ozil M, Emirik M, Belduz A, Ulker S (2016a) Molecular docking studies and synthesis of novel bisbenzimidazole derivatives as inhibitors of a-glucosidase. Bioorg Med Chem 24:5103–5114

Ozil M, Emirik M, Etlik SY, Ulke S, Kahveci B (2016b) A simple and efficient synthesis of novel inhibitors of alpha-glucosidase based on benzimidazole skeleton and molecular docking studies. Bioorg Chem 68:226–235

Özil M, Parlak C, Baltaş N (2016c) A simple and efficient synthesis of benzimidazoles containing piperazine or morpholine skeleton at C-6 position as glucosidase inhibitors with antioxidant activity. Bioorg Chem 76:468–477

Rekha S, Chandrashekhara S (2015) Antioxidant and antibacterial activities of thiazolidinedionederivatives. IJPSR 1:421–428

Scott LJ, Spencer CM (2000) Miglitol a review of its therapeutic potential in type 2 diabetes mellitus. Drugs 59:521–549

Singh A, Verma RK, Kuhad A, Mall R (2017) Novel indole-2-carboxylic acid linked 3-phenyl-2-alkoxy propanoic acids: synthesis, molecular docking and in vivo antidiabetic studies. Med Chem Res 26:745–759

Singh G, Singh A, Verma RK, Mall R, Azeem U (2018a) Synthesis, biological evaluation and molecular docking studies of novel benzimidazole derivatives. Comput Biol Chem 72:45–52

Singh V, Singh A, Singh G, Verma RK, Mall R (2018b) Novel benzoxazole derivatives featuring rhodanine and analogs as antihypergycemic agents: synthesis, molecular docking, and biological studies. Med Chem Res 27:735–743

Shahidpour S, Panahi F, Yousefi R, Nourisefat M, Nabipoor M, Nezhad AK (2015) Design and synthesis of new antidiabetic α-glucosidase and α-amylase inhibitors based on pyrimidine-fused heterocycles. Med chem Res 24:3086–3096

Tahaa M, Ismail NH, Imran S, Mohamad MH, Wadood A, Rahim F, Saad SM, Rehman A, Khan KM (2016) Synthesis, *α*-glucosidase inhibitory, cytotoxicity and docking studies of 2-aryl-7-methylbenzimidazoles. Bioorg Chem 65:100–109

Vallvee SG, Guasch L, Hernández ST, Bas JM, Ollendorff V, Arola L, Pujadas G, Mulero M (2015) Peroxisome proliferator-activated receptor γ (PPARγ) and ligand choreography: newcomers take the stage. J Med Chem 58:5381–5394

Verma RK, Ghosh P, Kumar V, Wadhwa LK (2012a) The application of comparative molecular field analysis for the design of α-anilino substituted-3-phenyl propanoic acids as novel PPARα/γ dual ligands. Med Chem Res 21:2873–2884

Verma RK, Kumar V, Ghosh P, Wadhwa LK (2012b) Heterocyclyl linked anilines and benzaldehydes as precursors for biologically significant new chemical entities. J Chem Sci 124: 1063–1069

Verma RK, Kumar V, Ghosh P, Wadhwa LK (2013b) 3D-QSAR study of tyrosine and propanoic acid derivatives as PPARα/γ dual agonists using CoMSIA. Med Chem Res 22:287–302

Verma RK, Mall R, Ghosh P, Kumar V(2013) Design and synthesis of benzimidazole-linked meta-substituted benzylidenes/benzyls as biologically significant new chemical entities Synth Commun 43:1882–1895

Verma RK, Mall R, Singh A (2015) Indolyl linked *meta*-substituted benzylidene-based novel PPAR ligands: synthetic and docking studies. Med Chem Res 24:1396–1407

Wang G, Chen M, Wang J, Peng Y, Li L, Xie ZZ, Deng B, Chen S, Li W (2017a) Synthesis, biological evaluation and molecular docking studies of chromone hydrazone derivatives as α-glucosidase inhibitors. Bioorg Med Chem Lett 27:2957–2961

Wang G, Peng Y, Xie Z, Wang J, Chen M (2017b) Synthesis, α-glucosidase inhibition and molecular docking studies of novel thiazolidine-2,4-dione or rhodanine derivatives. Med Chem Commun 8:1477–1484

West IC (2000) Radicals and oxidative stress in diabetes. Diabet Med 17:171–180

Yee HS, Fong NT (1996) A review of the safety and efficacy of Acarbose in diabetes mellitus. Pharmacotherapy 16:792–805

Yousefi A, Yousefi R, Panahi F, Sarikhani S, Zolghadr A, Bahaoddini A, Nezhad AK (2015) Novel curcumin-based pyrano[2,3-d]pyrimidine anti-oxidant inhibitors for α-amylase and α-glucosidase: implications for their pleiotropic effects against diabetes complications. Int J Biol Macromol 78:46–55

Zawawi NKNA, Taha M, Ahmat N, Ismail NH, Wadood A, Rahim F (2017) Synthesis, molecular docking studies of hybrid benzimidazole as *α*-glucosidase inhibitor. Bioorg Chem 70:184–191

Zawawi NKNA, Taha M, Ahmat N, Wadood A, Ismail NH, Rahim F, Azam SS, Abdullah N (2016) Benzimidazole derivatives as new α-glucosidase inhibitors and in silico studies. Bioorg Chem 64:29–36

Zhang B, Xing Y, Wen C, Yu X, Sun W, Xiu Z, Dong Y (2017) Pentacyclic triterpenes as α-glucosidase and α-amylase inhibitors: structure-activity relationships and the synergism with acarbose. Bioorg Med Chem Lett 27:5065–5070